

Massive MIMO with Dual-Polarized Antennas

Özgecan Özdoğan*, Emil Björnson*,[‡]

*Department of Electrical Engineering (ISY), Linköping University, Sweden

[‡]Department of Computer Science, KTH Royal Institute of Technology, Sweden

Email: ozgecan.ozdogan@liu.se, emilbjo@kth.se

Abstract

This paper considers a single-cell massive MIMO (multiple-input multiple-output) system with dual-polarized antennas at both the base station and users. We study a channel model that takes into account several practical aspects that arise when utilizing dual-polarization, such as channel cross-polar discrimination (XPD) and cross-polar correlations (XPC) at the transmitter and receiver. We analyze uplink and downlink achievable spectral efficiencies (SE) with and without successive interference cancellation (SIC) for the linear minimum mean squared error (MMSE), zero-forcing (ZF) and maximum ratio (MR) combining/precoding schemes. In addition, we derive the statistical properties of the MMSE channel estimator for the dual-polarized channel model. These estimates are used to implement different precoding and combining schemes when the uplink and downlink SE expressions are calculated for the case. Closed-form uplink and downlink SE expressions for MR combining/precoding are derived. Based on these results, we also provide power control algorithms to maximize the uplink and downlink sum SEs. Moreover, we compare the SEs achieved in dual-polarized and uni-polarized setups numerically and evaluate the impact of XPD and XPC.

Index Terms

Dual-polarized channels, Massive MIMO, power control.

I. INTRODUCTION

Massive MIMO (multiple-input multiple-output) is the key technology for increasing the spectral efficiency (SE) in 5G and beyond-5G cellular networks, by virtue of adaptive beamforming and spatial multiplexing [1]. A massive MIMO base station (BS) is equipped with a large number

This paper was supported by the Grant 2019-05068 from the Swedish Research Council.

of individually controllable antenna-integrated radios, which can be effectively used to serve tens of user equipments (UEs) on the same time-frequency resource. Wireless signals are polarized electromagnetic waves and there exist two orthogonal polarization dimensions. Practical BSs and UEs typically utilize dual-polarized antennas (i.e., two co-located antennas that respond to orthogonal polarizations) to squeeze in twice the number of antennas in the same physical enclosure [2], as well as capturing signal components from both dimensions for diversity and multiplexing purposes. Nevertheless, the main theory for massive MIMO has been developed for uni-polarized single-antenna users [3].

The channel modeling for dual-polarized channels is substantially more complicated than for conventional uni-polarized channels. Several measurements and channel models considering dual-polarized antennas are reported in prior literature. In [4], [5], the authors provide geometry-based channel models based on measurement campaigns for dual-polarized small-scale MIMO systems. In addition, [6], [7] provide analytical channel models based on extensive surveys of experimental results for single-user dual-polarized MIMO systems. The mentioned channel models are not equal, and therefore, there is no well-accepted single model. In this paper, we generalize the widely used model in [6] to a massive MIMO setup with multiple UEs. We select this model since it is analytically tractable, yet it includes the key effects of channel cross-polar discrimination (XPD), cross-polar receive and transmit correlations (XPC), and antenna polarization coupling commonly observed in measurements.

The capacity loss due to the polarization mismatch in a single-user dual-polarized MISO system is analyzed in [8]. In [9], a scenario with a massive MIMO BS with dual-polarized antennas and multiple users, each equipped with a uni-polarized single antenna, is considered. The system operates in frequency division duplex (FDD) mode and the users are grouped based on their spatial correlation matrices. The energy efficiency of a setup similar to [9] is evaluated in [10], while polarization leakage between the antennas is ignored (which makes the channels with different polarizations orthogonal). A distributed FDD massive MIMO system, where each user and distributed antenna port have a single uni-polarized antenna, is considered in [11]. A multi-user massive MIMO system with non-orthogonal multiple access is considered in [12]. The users are grouped so that the users that are in the same group share the same spatial correlation matrix, which is a simplifying assumption. Some other recent papers related to dual-polarized antennas are [13]–[15]. In [13] and [14], polarization-based modulation schemes are proposed. Furthermore, reconfigurable dual-polarized antennas that are able to change their

polarization states are considered in [13]. The authors in [15] consider the channel correlation matrix estimation problem.

The canonical form of massive MIMO operates in time-division duplex (TDD) mode and acquires channel state information (CSI) for uplink and downlink transmissions by using uplink pilot signaling and uplink-downlink channel reciprocity [3]. This paper evaluates the performance of such a single-cell massive MIMO network with multiple users operating in TDD mode. Different from the majority of previous works, both the BS and UEs are equipped with co-located dual-polarized antennas (as is common in practice). The main contributions are:

- We study a multi-user massive MIMO scenario with dual-polarized antennas at both the BS and UE sides, and spatial correlation at both sides by extending the channel model in [6]. To the best of our knowledge, this case has previously only been studied in the simplistic case with equal transmit spatial correlation matrices among the users [12].
- We analyze uplink and downlink achievable SEs with and without successive interference cancellation (SIC) for the linear minimum mean square error (MMSE), zero-forcing (ZF) and maximum ratio (MR) combining/precoding schemes.
- We derive the MMSE channel estimator and characterize its statistics. Using the estimates for MR combining/precoding, we compute closed-form uplink and downlink SE expressions.
- Based on the closed-form SE expressions, we provide power control algorithms to maximize the uplink and downlink sum SEs.
- The dual-polarized and uni-polarized antenna setups are compared numerically.
- The impact of XPD and XPC on uplink and downlink SEs are evaluated.

The conference version of this paper [16] only considered the downlink transmission with MMSE-SIC scheme and no power control.

Notation: Lower and upper case bold letters are used for vectors and matrices. The transpose and Hermitian transpose of a matrix \mathbf{A} are written as \mathbf{A}^T and \mathbf{A}^H , respectively. The superscript $(\cdot)^*$ denotes the complex conjugate operation. The $M \times M$ -dimensional matrix with the diagonal elements d_1, d_2, \dots, d_M is denoted as $\text{diag}(d_1, d_2, \dots, d_M)$. The diagonal elements of a matrix \mathbf{D} are extracted to a $M \times 1$ vector as $\text{diag}(\mathbf{D}) = [d_1, d_2, \dots, d_M]^T$. The expectation of a random variable X is denoted by $\mathbb{E}\{X\}$. The expectations are taken with respect to all sources of randomness.

II. SYSTEM MODEL WITH DUAL-POLARIZED ANTENNAS

We consider a single-cell massive MIMO system with $\frac{M}{2}$ dual-polarized antennas at the BS and K UEs, each equipped with a single dual-polarized antenna. Each dual-polarized antenna is composed of one vertical (V) and one horizontal (H) polarized antennas that are co-located.¹ A V/H polarized antenna emits and receives electromagnetic waves whose electric field oscillates in the V/H plane. Thus, the BS has M antennas in total and each UE has two antennas. Note that an array with a given aperture can accommodate twice as many antennas if dual-polarized antennas are utilized, compared to uni-polarized antennas. The system operates in TDD mode and we consider the standard block fading model [3], where the channels are static and frequency-flat within a coherence time-frequency block, and varies independently between blocks. We let τ_c denote the number of transmission samples per block.

Extending [6] and [8] to $\frac{M}{2}$ dual-polarized antennas and multiple UEs, the propagation channel of the UE k is

$$\begin{aligned} \mathbf{Z}_k &= \begin{bmatrix} \mathbf{Z}_{k1} & \mathbf{Z}_{k2} & \dots & \mathbf{Z}_{k\frac{M}{2}} \end{bmatrix} \in \mathbb{C}^{2 \times M} \\ &= \begin{bmatrix} z_{kV,1V} & z_{kV,1H} & z_{kV,2V} & z_{kV,2H} & \dots & z_{kV,\frac{M}{2}V} & z_{kV,\frac{M}{2}H} \\ z_{kH,1V} & z_{kH,1H} & z_{kH,2V} & z_{kH,2H} & \dots & z_{kH,\frac{M}{2}V} & z_{kH,\frac{M}{2}H} \end{bmatrix}, \end{aligned} \quad (1)$$

where $z_{kX,mY}$ is the channel coefficient between the X polarized component of the k th UE's dual-polarized antenna and Y polarized component of the m th dual-polarized BS antenna with $m \in 1, \dots, \frac{M}{2}$, $k \in 1, \dots, K$ and $X, Y \in \{V, H\}$. Therefore, each block $\mathbf{Z}_{km} \in \mathbb{C}^{2 \times 2}$ describes the relation from V to V , V to H , H to H and H to V polarized waves.

In free-space, the cross-polar transmissions (e.g., from a V polarized BS antenna to a H polarized UE antenna) is zero under ideal conditions. In a practical scenario, the propagation environment causes cross-polarization scattering that changes the initial polarization state of the electromagnetic waves on the way from the transmitter to the receiver. The channel cross-polarization discrimination (XPD) is the channel's ability to maintain radiated or received polarization purity between H and V polarized signals. We assume that it is independent of the BS antenna number m and define it for UE k as

$$\text{XPD}_k = \frac{\mathbb{E} \{ |z_{kV,mV}|^2 \}}{\mathbb{E} \{ |z_{kH,mV}|^2 \}} = \frac{\mathbb{E} \{ |z_{kH,mH}|^2 \}}{\mathbb{E} \{ |z_{kV,mH}|^2 \}} = \frac{1 - q_k}{q_k} \quad (2)$$

¹The analysis holds for any set of two orthogonally polarization directions. We just refer to them as V and H polarized for notational convenience.

for a coefficient $0 \leq q_k \leq 1$. By introducing this coefficient, we obtain

$$\mathbb{E} \{ |z_{kV,mV}|^2 \} = \mathbb{E} \{ |z_{kH,mH}|^2 \} = \beta_k (1 - q_k), \quad (3)$$

$$\mathbb{E} \{ |z_{kH,mV}|^2 \} = \mathbb{E} \{ |z_{kV,mH}|^2 \} = \beta_k q_k, \quad (4)$$

where β_k is the pathloss parameter of UE k . Small values of q_k (i.e., high channel XPD) are typically encountered in line-of-sight-dominated outdoor scenarios whereas low channel XPDs are observed in dense scattering environments [17]. It is important to note that (2) is different from the average ratio between the instantaneous values, i.e.,

$$\frac{\mathbb{E} \{ |z_{kV,mV}|^2 \}}{\mathbb{E} \{ |z_{kH,mV}|^2 \}} \neq \mathbb{E} \left\{ \frac{|z_{kV,mV}|^2}{|z_{kH,mV}|^2} \right\}. \quad (5)$$

Besides, the instantaneous variation between $|z_{kV,mV}|^2$ and $|z_{kH,mH}|^2$ can be as high as 10 dB due to the polarization selectivity feature of scattering environments [7], [18].

The polarization correlation matrices that define the correlation between the different polarization states are defined as [6]

$$\mathbf{C}_{\text{BS},k} = \begin{bmatrix} 1 & t_{p,k} \\ t_{p,k}^* & 1 \end{bmatrix} \quad \text{and} \quad \mathbf{C}_{\text{UE},k} = \begin{bmatrix} 1 & r_{p,k} \\ r_{p,k}^* & 1 \end{bmatrix}, \quad (6)$$

where the cross-polar correlation (XPC) terms $t_{p,k}$ and $r_{p,k}$ at the transmitter and receiver side are computed as

$$t_{p,k} = \frac{\mathbb{E} \{ z_{kV,mV} z_{kV,mH}^* \}}{\beta_k \sqrt{q_k (1 - q_k)}} = \frac{\mathbb{E} \{ z_{kH,mV} z_{kH,mH}^* \}}{\beta_k \sqrt{q_k (1 - q_k)}}, \quad (7)$$

$$r_{p,k} = \frac{\mathbb{E} \{ z_{kV,mV} z_{kH,mV}^* \}}{\beta_k \sqrt{q_k (1 - q_k)}} = \frac{\mathbb{E} \{ z_{kH,mH} z_{kV,mH}^* \}}{\beta_k \sqrt{q_k (1 - q_k)}}. \quad (8)$$

Various measurements indicate that the transmit and receiver XPCs are close to zero, see [19, Table 3.1]. Therefore, we assume that $t_{p,k} = r_{p,k} = 0$, i.e., $\mathbf{C}_{\text{BS},k} = \mathbf{C}_{\text{UE},k} = \mathbf{I}_2$ for the reason that V and H polarized waves fade independently through the channel [18]. The case when XPCs are non-zero is studied numerically in Section VII. Thus, each block in (1) can be written as

$$\mathbf{Z}_{km} = \boldsymbol{\Sigma}_k \odot \left(\mathbf{C}_{\text{UE},k}^{\frac{1}{2}} \mathbf{G}_{km} \mathbf{C}_{\text{BS},k}^{\frac{1}{2}} \right) = \boldsymbol{\Sigma}_k \odot \mathbf{G}_{km}, \quad (9)$$

where \odot is the Hadamard (element-wise) product,

$$\boldsymbol{\Sigma}_k = \begin{bmatrix} \sqrt{1 - q_k} & \sqrt{q_k} \\ \sqrt{q_k} & \sqrt{1 - q_k} \end{bmatrix}, \quad \mathbf{G}_{km} = \begin{bmatrix} g_{kV,mV} & g_{kV,mH} \\ g_{kH,mV} & g_{kH,mH} \end{bmatrix}, \quad (10)$$

and \mathbf{G}_{km} has i.i.d. circularly symmetric Gaussian entries with $g_{kX,mY} \sim \mathcal{N}_{\mathbb{C}}(0, \beta_k)$ for $X, Y \in \{V, H\}$. Eq. (9) expresses a 2×2 Rayleigh fading dual polarized MIMO channel. Each channel coefficient is scaled by the corresponding XPD coefficient and pathloss as the propagation environment dictates.

There are multiple dual-polarized antennas at the BS side. So, the spatial correlation of their fading should also be incorporated into the channel model. If we stack the elements related to UE k for different polarization combinations as $\mathbf{g}_{k,xy} = [g_{kx,1y}, \dots, g_{kx,\frac{M}{2}y}] \in \mathbb{C}^{\frac{M}{2} \times 1}$ with $x, y \in \{V, H\}$, then $\mathbf{g}_{k,xy} \sim \mathcal{N}_{\mathbb{C}}(\mathbf{0}, \mathbf{R}_{\text{BS},k})$ with the spatial correlation matrix $\mathbf{R}_{\text{BS},k} \in \mathbb{C}^{\frac{M}{2} \times \frac{M}{2}}$. For example, the vector $\mathbf{g}_{k,VH}$ denotes the relation (without the XPD coefficients) between the V polarized component of the UE k 's antenna and the H polarized component of the BS antennas. Since the V and H polarized antennas are co-located, they see the same scattering environment (in the statistical sense) and, therefore, all these vectors have the same spatial correlation matrix $\mathbf{R}_{\text{BS},k}$, i.e., $\mathbf{g}_{k,VV} \sim \mathcal{N}_{\mathbb{C}}(\mathbf{0}, \mathbf{R}_{\text{BS},k})$, $\mathbf{g}_{k,VH} \sim \mathcal{N}_{\mathbb{C}}(\mathbf{0}, \mathbf{R}_{\text{BS},k})$, $\mathbf{g}_{k,HV} \sim \mathcal{N}_{\mathbb{C}}(\mathbf{0}, \mathbf{R}_{\text{BS},k})$, and $\mathbf{g}_{k,HH} \sim \mathcal{N}_{\mathbb{C}}(\mathbf{0}, \mathbf{R}_{\text{BS},k})$. Since the two antennas at the UE side are co-located, the receiver spatial correlation matrix is simply $\mathbf{R}_{\text{UE},k} = \mathbf{I}_2, \forall k$. In summary, the propagation channel of UE k becomes

$$\begin{aligned} \mathbf{Z}_k &= \left(\mathbf{1}_{1 \times \frac{M}{2}} \otimes \boldsymbol{\Sigma}_k \right) \odot \left((\mathbf{R}_{\text{UE},k} \otimes \mathbf{C}_{\text{UE},k})^{1/2} \mathbf{S}_k (\mathbf{R}_{\text{BS},k} \otimes \mathbf{C}_{\text{BS},k})^{1/2} \right) \\ &= \left(\mathbf{1}_{1 \times \frac{M}{2}} \otimes \boldsymbol{\Sigma}_k \right) \odot \left(\mathbf{S}_k (\mathbf{R}_{\text{BS},k} \otimes \mathbf{I}_2)^{1/2} \right), \end{aligned} \quad (11)$$

where

$$\mathbf{S}_k = \begin{bmatrix} s_{kV,1V} & s_{kV,1H} & \dots & s_{kV,\frac{M}{2}V} & s_{kV,\frac{M}{2}H} \\ s_{kH,1V} & s_{kH,1H} & \dots & s_{kH,\frac{M}{2}V} & s_{kH,\frac{M}{2}H} \end{bmatrix} = \begin{bmatrix} \mathbf{s}_{kv} \\ \mathbf{s}_{kh} \end{bmatrix} \in \mathbb{C}^{2 \times M} \quad (12)$$

has i.i.d. entries with $\mathcal{N}_{\mathbb{C}}(0, 1)$ -distribution. The operator \otimes denotes the Kronecker product and it arises since the transmitter XPC term $t_{p,k} = 0$ is the same for each antenna element m and the receiver XPC coefficient $r_{p,k} = 0$ is equal for the H and V antenna elements of UE k .

The channel $\mathbf{H}_k \in \mathbb{C}^{2 \times M}$ including the BS and UE antenna hardware polarization effects is

$$\mathbf{H}_k = \mathbf{F}_{\text{UE},k} \mathbf{Z}_k \left(\mathbf{I}_{\frac{M}{2}} \otimes \mathbf{F}_{\text{BS}} \right), \quad (13)$$

where $\mathbf{F}_{\text{UE},k}$ and \mathbf{F}_{BS} are the deterministic polarization matrices at the UE k and BS, respectively. The polarization matrices are modeled by $[\mathbf{f}_1, \mathbf{f}_2]$ where \mathbf{f}_1 and \mathbf{f}_2 are unit norm vectors corresponding to the polarization ports (V/H) [6]. If \mathbf{f}_1 and \mathbf{f}_2 are mutually orthogonal then there is no polarization coupling between the two orthogonally polarized ports. On the other hand, for

imperfect antennas, these vectors may have a nonzero parallelity term $p = |\mathbf{f}_1^H \mathbf{f}_2|$. In this case, the dual-polarized antenna experiences a polarization coupling loss. To account for this loss, the polarization matrix is scaled as [6]

$$\mathbf{F} = \frac{1}{\sqrt{1+p}} [\mathbf{f}_1, \mathbf{f}_2]. \quad (14)$$

The ratio of the power coupled between the V and H antennas of a dual-polarized antenna is determined by the antenna's cross-polar isolation (XPI) ability. The XPI is a quality metric of antennas and it is defined as the ratio of the desired co-polar and undesired cross-polar power levels radiated/received from an antenna [20]. For simplicity, we assume that the antenna hardware can perfectly isolate the polarization states such that $\mathbf{F}_{\text{UE},k} = \mathbf{F}_{\text{BS}} = \mathbf{I}_2$.²

Then, we can write (13) as

$$\begin{aligned} \mathbf{H}_k &= \mathbf{F}_{\text{UE},k} \mathbf{Z}_k \left(\mathbf{I}_{\frac{M}{2}} \otimes \mathbf{F}_{\text{BS}} \right) \\ &= \left(\mathbf{1}_{1 \times \frac{M}{2}} \otimes \boldsymbol{\Sigma}_k \right) \odot \left(\mathbf{S}_k \left(\mathbf{R}_{\text{BS},k} \otimes \mathbf{I}_2 \right)^{1/2} \right) \\ &= \left[\left(\mathbf{1}_{1 \times \frac{M}{2}} \otimes \boldsymbol{\Sigma}_k \right) \odot \mathbf{S}_k \right] \mathbf{R}_k^{1/2} \\ &= \begin{bmatrix} \tilde{s}_{kV,1V} & \tilde{s}_{kV,1H} & \cdots & \tilde{s}_{kV,\frac{M}{2}V} & \tilde{s}_{kV,\frac{M}{2}H} \\ \tilde{s}_{kH,1V} & \tilde{s}_{kH,1H} & \cdots & \tilde{s}_{kH,\frac{M}{2}V} & \tilde{s}_{kH,\frac{M}{2}H} \end{bmatrix} \mathbf{R}_k^{1/2} \\ &\triangleq \tilde{\mathbf{S}}_k \mathbf{R}_k^{1/2}, \end{aligned} \quad (15)$$

where $\mathbf{R}_k = \mathbf{R}_{\text{BS},k} \otimes \mathbf{I}_2$ and $\tilde{\mathbf{S}}_k = \left(\mathbf{1}_{1 \times \frac{M}{2}} \otimes \boldsymbol{\Sigma}_k \right) \odot \mathbf{S}_k = \begin{bmatrix} \tilde{s}_{kV} & \tilde{s}_{kH} \end{bmatrix}^H$. Notice that $\mathbb{E} \{ |\tilde{s}_{kV,mV}|^2 \} = \mathbb{E} \{ |\tilde{s}_{kH,mH}|^2 \} = 1 - q_k$ and $\mathbb{E} \{ |\tilde{s}_{kV,mH}|^2 \} = \mathbb{E} \{ |\tilde{s}_{kH,mV}|^2 \} = q_k$ and they have zero mean. Then, $\mathbf{H}_k = \begin{bmatrix} \mathbf{h}_{kV} & \mathbf{h}_{kH} \end{bmatrix}^H \in \mathbb{C}^{2 \times M}$ where the row vectors show the channels between the V and H components of UE k and all BS antennas:

$$\mathbf{h}_{kV} = \mathbf{R}_k^{1/2} \tilde{\mathbf{s}}_{kV} \in \mathbb{C}^{M \times 1}, \quad (16)$$

$$\mathbf{h}_{kH} = \mathbf{R}_k^{1/2} \tilde{\mathbf{s}}_{kH} \in \mathbb{C}^{M \times 1}. \quad (17)$$

²For well-designed antennas, the antenna depolarization effects can be minimized (for example, XPIs on the order of 30 dBs or more) compared to the propagation channel depolarization effects [21, Chapter 8].

The covariance matrices of these matrices will be utilized during the channel estimation and are computed as

$$\mathbb{E} \{ \mathbf{h}_{kV} \mathbf{h}_{kV}^H \} = \mathbf{R}_k^{1/2} \begin{bmatrix} 1 - q_k & 0 & \dots & 0 \\ 0 & q_k & & \\ \vdots & & \ddots & \vdots \\ & & & 1 - q_k & 0 \\ 0 & \dots & & 0 & q_k \end{bmatrix} \left(\mathbf{R}_k^{1/2} \right)^H \triangleq \mathbf{R}_k^v, \quad (18)$$

and

$$\mathbb{E} \{ \mathbf{h}_{kH} \mathbf{h}_{kH}^H \} = \mathbf{R}_k^{1/2} \begin{bmatrix} q_k & 0 & \dots & 0 \\ 0 & 1 - q_k & & \\ \vdots & & \ddots & \vdots \\ & & & q_k & 0 \\ 0 & \dots & & 0 & 1 - q_k \end{bmatrix} \left(\mathbf{R}_k^{1/2} \right)^H \triangleq \mathbf{R}_k^h, \quad (19)$$

where $\mathbf{R}_k^v + \mathbf{R}_k^h = \mathbf{R}_k$. Besides, we calculate

$$\mathbb{E} \left\{ \text{vec}(\mathbf{H}_k^H) \text{vec}(\mathbf{H}_k^H)^H \right\} = \begin{bmatrix} \mathbf{R}_k^v & \mathbf{0} \\ \mathbf{0} & \mathbf{R}_k^h \end{bmatrix} \triangleq \mathbf{R}_{bk} \in \mathbb{C}^{2M \times 2M}, \quad (20)$$

where $\text{vec}(\cdot)$ denotes vectorization. Notice that (20) implies $\mathbb{E} \{ \mathbf{h}_{kH} \mathbf{h}_{kV}^H \} = \mathbb{E} \{ \mathbf{h}_{kV} \mathbf{h}_{kH}^H \} = \mathbf{0}$ since the V and H polarized waves fade independently through the channel.

III. CHANNEL ESTIMATION

Each BS requires CSI for uplink receive processing and downlink transmit precoding. Therefore, τ_p samples are reserved for performing uplink pilot-based channel estimation in each coherence block, giving room for τ_p mutually orthogonal pilot sequences. Following [22], [23], each UE sends its pilot signal $\Phi_k \in \mathbb{C}^{2 \times \tau_p}$ to the BS with $\tau_p = 2K$ (and $2K \leq \tau_c$) to estimate all channel dimensions at the BS. The pilot signal is designed as $\Phi_k = \mathbf{L}_k^{1/2} \mathbf{V}_k^T$ where $\mathbf{L}_k = \text{diag}(p_{kV}, p_{kH})$ is a pilot allocation matrix with p_{kV}, p_{kH} being the pilot powers allocated to the V and H polarized antennas, respectively. The orthogonal pilot matrix $\mathbf{V}_k \in \mathbb{C}^{2 \times \tau_p}$ is designed so that $\mathbf{V}_k^H \mathbf{V}_k = \tau_p \mathbf{I}_2$ and $\mathbf{V}_k^H \mathbf{V}_l = \mathbf{0}_2$ if $l \neq k$. Also, $\text{tr}(\Phi_k \Phi_k^H) / \tau_p \leq P_k$ where P_k is the total uplink pilot power of UE k . Thus,

$$\Phi_k \mathbf{V}_k^* = \begin{bmatrix} \sqrt{p_{kV} \tau_p} & 0 \\ 0 & \sqrt{p_{kH} \tau_p} \end{bmatrix} = \tau_p \mathbf{L}_k^{1/2}, \quad (21)$$

$$\Phi_k \mathbf{V}_l^* = \mathbf{0}_2, \quad l \neq k. \quad (22)$$

All UEs transmit their pilot signals simultaneously. The received pilot signal $\mathbf{Y} \in \mathbb{C}^{M \times \tau_p}$ at the BS is then given by

$$\mathbf{Y} = \sum_{l=1}^K \mathbf{H}_l^H \Phi_l + \mathbf{N}, \quad (23)$$

where $\text{vec}(\mathbf{N}) \sim \mathcal{N}_{\mathbb{C}}(\mathbf{0}, \sigma_{\text{ul}}^2 \mathbf{I}_{M\tau_p})$ is the receiver noise with variance σ_{ul}^2 . To estimate the channel of UE k , the BS can first process the receive signal by correlating it with the UE's pilot signal.

The processed pilot signal $\mathbf{Y}_k^p \in \mathbb{C}^{M \times 2}$ is

$$\mathbf{Y}_k^p = \mathbf{Y} \mathbf{V}_k^* = \tau_p \mathbf{H}_k^H \mathbf{L}_k^{1/2} + \mathbf{N} \mathbf{V}_k^*. \quad (24)$$

Vectorizing (24) gives

$$\text{vec}(\mathbf{Y}_k^p) = \mathbf{A} \text{vec}(\mathbf{H}_k^H) + \text{vec}(\mathbf{N} \mathbf{V}_k^*), \quad (25)$$

where $\mathbf{A} = (\tau_p \mathbf{L}_k^{1/2} \otimes \mathbf{I}_M)$ and $\text{vec}(\mathbf{N} \mathbf{V}_k^*) \sim \mathcal{N}_{\mathbb{C}}(\mathbf{0}, \sigma_{\text{ul}}^2 \tau_p \mathbf{I}_{2M})$. Besides, the received processed

pilot signal can be written as $\text{vec}(\mathbf{Y}_k^p) \triangleq \begin{bmatrix} \mathbf{y}_{kV}^p \\ \mathbf{y}_{kH}^p \end{bmatrix}$ where

$$\mathbb{E} \{ \mathbf{y}_{kV}^p (\mathbf{y}_{kV}^p)^H \} = \tau_p (p_{kV} \tau_p \mathbf{R}_k^v + \sigma_{\text{ul}}^2 \mathbf{I}_M) \triangleq \tau_p (\Psi_k^v)^{-1}, \quad (26)$$

$$\mathbb{E} \{ \mathbf{y}_{kH}^p (\mathbf{y}_{kH}^p)^H \} = \tau_p (p_{kH} \tau_p \mathbf{R}_k^h + \sigma_{\text{ul}}^2 \mathbf{I}_M) \triangleq \tau_p (\Psi_k^h)^{-1}. \quad (27)$$

Then, based on (25), the MMSE estimate of \mathbf{H}_k is [23]

$$\begin{aligned} \text{vec}(\hat{\mathbf{H}}_k^H) &= \mathbf{R}_{bk} \mathbf{A}^H (\mathbf{A} \mathbf{R}_{bk} \mathbf{A}^H + \sigma_{\text{ul}}^2 \tau_p \mathbf{I}_{2M})^{-1} \text{vec}(\mathbf{Y}_k^p) \\ &= \begin{bmatrix} \sqrt{p_{kV}} \mathbf{R}_k^v \Psi_k^v \mathbf{y}_{kV}^p \\ \sqrt{p_{kH}} \mathbf{R}_k^h \Psi_k^h \mathbf{y}_{kH}^p \end{bmatrix} \triangleq \begin{bmatrix} \hat{\mathbf{h}}_{kV} \\ \hat{\mathbf{h}}_{kH} \end{bmatrix}, \end{aligned} \quad (28)$$

where the MMSE estimates associated with V/H antennas are uncorrelated random variables:

$$\hat{\mathbf{h}}_{kV} \sim \mathcal{N}_{\mathbb{C}}(\mathbf{0}, \mathbf{\Gamma}_k^v), \quad (29)$$

$$\hat{\mathbf{h}}_{kH} \sim \mathcal{N}_{\mathbb{C}}(\mathbf{0}, \mathbf{\Gamma}_k^h), \quad (30)$$

with $\mathbf{\Gamma}_k^v = p_{kV}\tau_p\mathbf{R}_k^v\Psi_k^v\mathbf{R}_k^v$ and $\mathbf{\Gamma}_k^h = p_{kH}\tau_p\mathbf{R}_k^h\Psi_k^h\mathbf{R}_k^h$ where $\text{tr}(\mathbf{\Gamma}_k^v) = \text{tr}(\mathbf{\Gamma}_k^h)$ for equal pilot powers $p_{kV} = p_{kH}$. Note that the estimates $\hat{\mathbf{h}}_{kV}$ and $\hat{\mathbf{h}}_{kH}$ are uncorrelated since the channels \mathbf{h}_{kV} and \mathbf{h}_{kH} are uncorrelated. The error covariance matrix is

$$\begin{aligned} \mathbf{C}_{\text{MMSE},k} &= \mathbf{R}_{bk} - \mathbf{R}_{bk}\mathbf{A}^H (\mathbf{A}\mathbf{R}_{bk}\mathbf{A}^H + \sigma_{\text{ul}}^2\tau_p\mathbf{I}_{2M})^{-1} \mathbf{A}\mathbf{R}_{bk} \\ &= \begin{bmatrix} \mathbf{R}_k^v - \mathbf{\Gamma}_k^v & \mathbf{0} \\ \mathbf{0} & \mathbf{R}_k^h - \mathbf{\Gamma}_k^h \end{bmatrix} \triangleq \begin{bmatrix} \mathbf{C}_k^v & \mathbf{0} \\ \mathbf{0} & \mathbf{C}_k^h \end{bmatrix}. \end{aligned} \quad (31)$$

These results will be utilized in the uplink and downlink transmissions to design combining and precoding schemes.

IV. UPLINK TRANSMISSION

In the uplink data transmission phase, the received signal at the BS is

$$\mathbf{y} = \sum_{l=1}^K \mathbf{H}_l^H \mathbf{P}_l^{1/2} \mathbf{x}_l + \mathbf{n}, \quad (32)$$

where $\mathbf{P}_l = \begin{bmatrix} \rho_{lV}^{\text{ul}} & 0 \\ 0 & \rho_{lH}^{\text{ul}} \end{bmatrix}$ is the uplink transmit power allocation matrix, $\mathbf{x}_l = \begin{bmatrix} x_{lV} \\ x_{lH} \end{bmatrix} \sim \mathcal{N}_{\mathbb{C}}(\mathbf{0}, \mathbf{I}_2)$ is the data signals and $\mathbf{n} \sim \mathcal{N}_{\mathbb{C}}(\mathbf{0}, \sigma_{\text{ul}}^2\mathbf{I}_M)$ is the receiver noise. According to the block-fading assumption, at the beginning of each coherence block, the channels realizations are unknown. Then, in the channel estimation phase of the TDD operation, the channels are estimated at the BS side and the UEs do not have instantaneous CSIs. Therefore, the precoder matrix of user k is selected as an identity matrix in (32) to send one signal per polarization.

A. Uplink Linear Detection

First, we consider the case in which the data signals from each UE antenna, x_{lV} and x_{lH} , are decoded simultaneously while treating the other streams as noise. A linear detector $\mathbf{v}_{ki} \in \mathbb{C}^{M \times 1}$ for $i \in \{V, H\}$ based on the channel estimates is applied to the received signal as

$$\mathbf{v}_{ki}^H \mathbf{y} = \sum_{l=1}^K \sqrt{\rho_{lV}^{\text{ul}}} \mathbf{v}_{ki}^H \mathbf{h}_{lV} x_{lV} + \sqrt{\rho_{lH}^{\text{ul}}} \mathbf{v}_{ki}^H \mathbf{h}_{lH} x_{lH} + \mathbf{v}_{ki}^H \mathbf{n}. \quad (33)$$

Then, we can rewrite (33) as

$$\begin{aligned} \mathbf{v}_{ki}^H \mathbf{y} &= \sqrt{\rho_{ki}^{\text{ul}}} \mathbb{E} \{ \mathbf{v}_{ki}^H \mathbf{h}_{ki} \} x_{ki} + \sqrt{\rho_{ki}^{\text{ul}}} (\mathbf{v}_{ki}^H \mathbf{h}_{ki} - \mathbb{E} \{ \mathbf{v}_{ki}^H \mathbf{h}_{ki} \}) x_{ki} \\ &+ \sqrt{\rho_{ki'}^{\text{ul}}} \mathbf{v}_{ki'}^H \mathbf{h}_{ki'} x_{ki'} + \sum_{l \neq k} \sqrt{\rho_{lV}^{\text{ul}}} \mathbf{v}_{ki}^H \mathbf{h}_{lV} x_{lV} + \sqrt{\rho_{lH}^{\text{ul}}} \mathbf{v}_{ki}^H \mathbf{h}_{lH} x_{lH} + \mathbf{v}_{ki}^H \mathbf{n}, \end{aligned} \quad (34)$$

by adding and subtracting the averaged precoded channel $\mathbb{E}\{\mathbf{v}_{ki}^H \mathbf{h}_{ki}\}$. Let i' denote the opposite polarization so that $i \cup i' = \{V, H\}$ and $i \neq i'$. The desired signal received over the averaged precoded channel $\mathbb{E}\{\mathbf{v}_{ki}^H \mathbf{h}_{ki}\}$ is treated as the true desired signal. The part received over $(\mathbf{v}_{ki}^H \mathbf{h}_{ki} - \mathbb{E}\{\mathbf{v}_{ki}^H \mathbf{h}_{ki}\})$ is treated as uncorrelated noise. The following lemma provides a lower bound on the uplink capacity, which makes it an achievable SE. This bound is referred to as the use-and-then-forget (UaTF) [3] since the channel estimates are utilized in the receiver combining and then forgotten before the signal detection.

Lemma 1: The uplink achievable SE of UE k using the UaTF bound is

$$R_k^{\text{ul}} = \frac{\tau_c - \tau_p}{\tau_c} \sum_{i \in \{V, H\}} \log_2(1 + \gamma_{ki}) \quad (35)$$

with

$$\gamma_{ki} = \frac{\rho_{ki}^{\text{ul}} |\mathbb{E}\{\mathbf{v}_{ki}^H \mathbf{h}_{ki}\}|^2}{\sum_{l=1}^K \rho_{lV}^{\text{ul}} \mathbb{E}\{|\mathbf{v}_{ki}^H \mathbf{h}_{lV}|^2\} + \rho_{lH}^{\text{ul}} \mathbb{E}\{|\mathbf{v}_{ki}^H \mathbf{h}_{lH}|^2\} - \rho_{ki}^{\text{ul}} |\mathbb{E}\{\mathbf{v}_{ki}^H \mathbf{h}_{ki}\}|^2 + \sigma_{\text{ul}}^2 \mathbb{E}\{\|\mathbf{v}_{ki}\|^2\}}. \quad (36)$$

Proof: The derivation is similar to that in [3, Theorem 4.4] and is therefore omitted. \square

The uplink achievable SE in (35) can be computed for any choice of combining vector. The MMSE detector is

$$\mathbf{v}_{ki}^{\text{MMSE}} = \sqrt{\rho_{ki}^{\text{ul}}} \mathbf{\Upsilon}^{-1} \hat{\mathbf{h}}_{ki}, \quad (37)$$

where $\mathbf{\Upsilon} = \sum_{l=1}^K \hat{\mathbf{H}}_l^H \mathbf{P}_l \hat{\mathbf{H}}_l + \rho_{lV}^{\text{ul}} \mathbf{C}_l^v + \rho_{lH}^{\text{ul}} \mathbf{C}_l^h + \sigma_{\text{ul}}^2 \mathbf{I}_M$. Other potential selections of \mathbf{v}_{ki} for low complexity can be ZF and MR combining vectors as

$$\mathbf{v}_{ki}^{\text{ZF}} = \left[\hat{\mathbf{H}}_{\text{all}} \left(\hat{\mathbf{H}}_{\text{all}}^H \hat{\mathbf{H}}_{\text{all}} \right)^{-1} \right]_{ki}, \quad (38)$$

$$\mathbf{v}_{ki}^{\text{MR}} = \hat{\mathbf{h}}_{ki}, \quad (39)$$

where $\hat{\mathbf{H}}_{\text{all}} = [\hat{\mathbf{H}}_1^H, \dots, \hat{\mathbf{H}}_K^H] = [\hat{\mathbf{h}}_{1V} \ \hat{\mathbf{h}}_{1H}, \dots, \hat{\mathbf{h}}_{KV} \ \hat{\mathbf{h}}_{KH}] \in \mathbb{C}^{M \times 2K}$ and $[\cdot]_{ki}$ denotes the k^{th} column corresponds to k^{th} UE and $i \in \{V, H\}$. It is expected that MR combining will provide lower SEs than the other combining vectors but it does not require any matrix inversion. In the following lemma, (35) is computed in closed form for MR combining.

Lemma 2: If MR combining $\mathbf{v}_{ki}^{\text{MR}} = \hat{\mathbf{h}}_{ki}$ is used based on the MMSE estimator, then the achievable SE in (35) can be computed in closed form as

$$\begin{aligned}
R_k^{\text{ul}} &= \frac{\tau_c - \tau_p}{\tau_c} \log_2 \left(1 + \frac{\rho_{kV}^{\text{ul}} \text{tr}(\mathbf{\Gamma}_k^v)}{\sum_{l=1}^K \left(\rho_{lV}^{\text{ul}} \frac{\text{tr}(\mathbf{\Gamma}_k^v \mathbf{R}_l^v)}{\text{tr}(\mathbf{\Gamma}_k^v)} + \rho_{lH}^{\text{ul}} \frac{\text{tr}(\mathbf{\Gamma}_k^v \mathbf{R}_l^h)}{\text{tr}(\mathbf{\Gamma}_k^v)} \right) + \sigma_{\text{ul}}^2} \right) \\
&+ \frac{\tau_c - \tau_p}{\tau_c} \log_2 \left(1 + \frac{\rho_{kH}^{\text{ul}} \text{tr}(\mathbf{\Gamma}_k^h)}{\sum_{l=1}^K \left(\rho_{lH}^{\text{ul}} \frac{\text{tr}(\mathbf{\Gamma}_k^h \mathbf{R}_l^h)}{\text{tr}(\mathbf{\Gamma}_k^h)} + \rho_{lV}^{\text{ul}} \frac{\text{tr}(\mathbf{\Gamma}_k^h \mathbf{R}_l^v)}{\text{tr}(\mathbf{\Gamma}_k^h)} \right) + \sigma_{\text{ul}}^2} \right). \quad (40)
\end{aligned}$$

Proof: Similar to Appendix B. \square

The closed-form expression in (40) provides insights into the basic behaviors of dual-polarized massive MIMO. The first and second logarithms correspond to the data streams associated with V/H polarizations, respectively. The signal terms in the numerator depend on the channel estimation quality. The denominators contain the interference terms. The simplified version of (40) for spatially uncorrelated channels, $\mathbf{R}_{\text{BS},k} = \beta_k \mathbf{I}_{\frac{M}{2}}$ for $k = 1, \dots, K$, is

$$\begin{aligned}
R_k^{\text{ul}} &= \frac{\tau_c - \tau_p}{\tau_c} \log_2 \left(1 + \frac{\frac{M}{2} \rho_{kV}^{\text{ul}} (\gamma_{kV,1} + \gamma_{kV,2})}{\sum_{l=1}^K \left(\rho_{lV}^{\text{ul}} \frac{\gamma_{kV,1} \beta_l (1 - q_l) + \gamma_{kV,2} \beta_l q_l}{\gamma_{kV,1} + \gamma_{kV,2}} + \rho_{lH}^{\text{ul}} \frac{\gamma_{kV,1} \beta_l q_l + \gamma_{kV,2} \beta_l (1 - q_l)}{\gamma_{kV,1} + \gamma_{kV,2}} \right) + \sigma_{\text{ul}}^2} \right) \\
&+ \frac{\tau_c - \tau_p}{\tau_c} \log_2 \left(1 + \frac{\frac{M}{2} \rho_{kH}^{\text{ul}} (\gamma_{kH,1} + \gamma_{kH,2})}{\sum_{l=1}^K \left(\rho_{lH}^{\text{ul}} \frac{\gamma_{kH,1} \beta_l (1 - q_l) + \gamma_{kH,2} \beta_l q_l}{\gamma_{kH,1} + \gamma_{kH,2}} + \rho_{lV}^{\text{ul}} \frac{\gamma_{kH,1} \beta_l q_l + \gamma_{kH,2} \beta_l (1 - q_l)}{\gamma_{kH,1} + \gamma_{kH,2}} \right) + \sigma_{\text{ul}}^2} \right), \quad (41)
\end{aligned}$$

where $\gamma_{kV,1} = \frac{p_{kV} \tau_p \beta_k^2 (1 - q_k)^2}{p_{kV} \tau_p \beta_k (1 - q_k) + \sigma_{\text{ul}}^2}$, $\gamma_{kV,2} = \frac{p_{kV} \tau_p \beta_k^2 q_k^2}{p_{kV} \tau_p \beta_k q_k + \sigma_{\text{ul}}^2}$, $\gamma_{kH,1} = \frac{p_{kH} \tau_p \beta_k^2 (1 - q_k)^2}{p_{kH} \tau_p \beta_k (1 - q_k) + \sigma_{\text{ul}}^2}$ and $\gamma_{kH,2} = \frac{p_{kH} \tau_p \beta_k^2 q_k^2}{p_{kH} \tau_p \beta_k q_k + \sigma_{\text{ul}}^2}$. Notice that there is an array gain of $\frac{M}{2}$ for each data stream, equal to the number of antennas per polarization. Besides, the interference terms are non-coherent since they do not scale with the number of antennas and are products of the data transmission powers and channel gains. The general SE expression in (40) can be also interpreted in a similar way by noticing that each trace expression is proportional to $\frac{M}{2}$, while ratios of traces are not scaling with M .

B. Uplink MMSE-SIC detection

Using the linear detection method above, we observe that the self-interference that is caused by the data stream corresponding to the opposite polarization at the same UE is not suppressed.

Alternatively, the UE may apply an MMSE successive interference cancellation (SIC) detector to detect the streams since the BS has the estimated channels $\hat{\mathbf{H}}_1, \dots, \hat{\mathbf{H}}_K$. The lower bound on the uplink SE when the MMSE-SIC scheme is used is given in the following lemma.

Lemma 3: Using per-stream MMSE-SIC decoding at the BS, the achievable SE of UE k using MMSE-SIC is

$$R_k^{\text{ul,SIC}} = \frac{\tau_c - \tau_p}{\tau_c} \mathbb{E} \left\{ \log_2 \det \left(\mathbf{I}_2 + \mathbf{P}_k \hat{\mathbf{H}}_k \left(\sum_{l=k+1}^K \rho_{lV}^{\text{ul}} \hat{\mathbf{h}}_{lV} \hat{\mathbf{h}}_{lV}^H + \rho_{lH}^{\text{ul}} \hat{\mathbf{h}}_{lH} \hat{\mathbf{h}}_{lH}^H + \sum_{l=1}^K \rho_{lV}^{\text{ul}} \mathbf{C}_l^v + \rho_{lH}^{\text{ul}} \mathbf{C}_l^h + \sigma_{\text{ul}}^2 \mathbf{I}_M \right)^{-1} \hat{\mathbf{H}}_k^H \right) \right\}, \quad (42)$$

and the achievable uplink sum SE is

$$R^{\text{ul,SIC}} = \sum_{l=1}^K R_l^{\text{ul,SIC}} = \frac{\tau_c - \tau_p}{\tau_c} \mathbb{E} \left\{ \log_2 \det \left(\mathbf{I}_M + \sum_{l=1}^K \hat{\mathbf{H}}_l^H \mathbf{P}_l \hat{\mathbf{H}}_l \left(\sum_{j=1}^K \rho_{jV}^{\text{ul}} \mathbf{C}_j^v + \rho_{jH}^{\text{ul}} \mathbf{C}_j^h + \sigma_{\text{ul}}^2 \mathbf{I}_M \right)^{-1} \right) \right\}. \quad (43)$$

Proof: The proof is given in Appendix A. \square

The MMSE-SIC procedure may be a computationally heavy process depending on the number of streams since the signals need to be buffered.

V. DOWNLINK TRANSMISSION

In the downlink data transmission, the BS transmits simultaneously to all UEs using precoding computed based on the channel estimates derived in Section III. The transmitted downlink signal is

$$\mathbf{x} = \sum_{l=1}^K \mathbf{W}_l \mathbf{d}_l, \quad (44)$$

where $\mathbf{d}_l \in \mathbb{C}^{2 \times 1}$ is the transmit signal satisfying $\mathbb{E} \{ \mathbf{d}_l \mathbf{d}_l^H \} = \mathbf{I}_2$ and $\mathbf{W}_l \in \mathbb{C}^{M \times 2}$ is the downlink precoding matrix such that $\text{tr} (\mathbb{E} \{ \mathbf{W}_l^H \mathbf{W}_l \}) \leq \rho_{lV}^{\text{dl}} + \rho_{lH}^{\text{dl}}$ where the transmit powers of V/H the antennas are denoted ρ_{lV}^{dl} and ρ_{lH}^{dl} , respectively.

The received signal at UE k is denoted by $\mathbf{y}_k \in \mathbb{C}^{2 \times 1}$ and computed as

$$\mathbf{y}_k = \mathbf{H}_k \mathbf{x} + \mathbf{n}_k = \mathbf{H}_k \mathbf{W}_k \mathbf{d}_k + \mathbf{H}_k \sum_{\substack{l=1 \\ l \neq k}}^K \mathbf{W}_l \mathbf{d}_l + \mathbf{n}_k, \quad (45)$$

where $\mathbf{n}_k \sim \mathcal{N}_{\mathbb{C}}(\mathbf{0}, \sigma_{\text{dl}}^2 \mathbf{I}_2)$ is the receiver noise. The first term in (45) corresponds to the desired signal whereas the second term is the interference caused by transmissions to other users.

A. Downlink Linear Processing

The UEs do not have instantaneous CSIs since no downlink pilots are sent. However, their average effective channels $\mathbb{E}\{\mathbf{H}_k \mathbf{W}_k\}$ are known. The UEs can detect each data symbol separately using the linear MMSE combining vector $\mathbf{v}_{dl,ki} \in \mathbb{C}^{2 \times 1}$ as [22]

$$\mathbf{v}_{dl,ki} = \left(\mathbb{E} \left\{ \mathbf{H}_k \sum_{l=1}^K \mathbf{W}_l \mathbf{W}_l^H \mathbf{H}_k^H \right\} + \sigma_{dl}^2 \mathbf{I}_2 \right)^{-1} [\mathbb{E}\{\mathbf{H}_k \mathbf{W}_k\}]_{ki} \quad (46)$$

for $i \in \{V, H\}$ to the received signal (45). Similar to [22], we have the following result.

Lemma 4: An achievable downlink SE is

$$R_k^{\text{woSIC}} = \frac{\tau_c - \tau_p}{\tau_c} \sum_{i \in \{V, H\}} \log_2 (1 + \eta_{ki}^{\text{dl}}), \quad (47)$$

where the SINR η_{ki}^{dl} is

$$\eta_{ki}^{\text{dl}} = \frac{|\mathbf{v}_{dl,ki}^H [\mathbb{E}\{\mathbf{H}_k \mathbf{W}_k\}]_{ki}|^2}{\mathbf{v}_{dl,ki}^H \left(\mathbb{E} \left\{ \mathbf{H}_k \sum_{l=1}^K \mathbf{W}_l \mathbf{W}_l^H \mathbf{H}_k^H \right\} + \sigma_{dl}^2 \mathbf{I}_2 - [\mathbb{E}\{\mathbf{H}_k \mathbf{W}_k\}]_{ki} [\mathbb{E}\{\mathbf{H}_k \mathbf{W}_k\}]_{ki}^H \right) \mathbf{v}_{dl,ki}}. \quad (48)$$

This SE expression can be computed for any choice of precoding and combining vectors. However, the linear MMSE combining vector in (46) maximizes it for given precoding vectors.

B. Downlink MMSE-SIC Processing

Similar to the uplink, the MMSE-SIC scheme can be used to detect signals. The following lemma gives a lower bound on the downlink capacity which makes it an achievable SE.

Lemma 5: An achievable downlink SE of UE k using MMSE-SIC detection is [22, Theorem 2]

$$R_k^{\text{dl}} = \frac{\tau_c - \tau_p}{\tau_c} \log_2 \det \left(\mathbf{I}_2 + (\mathbb{E}\{\mathbf{H}_k \mathbf{W}_k\})^H \mathbf{\Omega}_k \mathbb{E}\{\mathbf{H}_k \mathbf{W}_k\} \right), \quad (49)$$

where

$$\mathbf{\Omega}_k = \left(\mathbb{E} \left\{ \mathbf{H}_k \sum_{l=1}^K \mathbf{W}_l \mathbf{W}_l^H \mathbf{H}_k^H \right\} + \sigma_{dl}^2 \mathbf{I}_2 - \mathbb{E}\{\mathbf{H}_k \mathbf{W}_k\} (\mathbb{E}\{\mathbf{H}_k \mathbf{W}_k\})^H \right)^{-1}. \quad (50)$$

Proof: This bound can be achieved if UE k applies MMSE-SIC detection to \mathbf{y}_k by treating $\mathbb{E}\{\mathbf{H}_k \mathbf{W}_k\}$ as the true channel and the uncorrelated term $\mathbf{y}_k - \mathbb{E}\{\mathbf{H}_k \mathbf{W}_k\} \mathbf{d}_k$ as independent noise. \square

The rate expression can be computed numerically for any choice of precoding. We consider three linear precoders \mathbf{W}_k , namely linear MMSE, zero-forcing and MR that are defined as

$$\mathbf{W}_k^X = \begin{bmatrix} \frac{\mathbf{v}_{kV}^X}{\sqrt{\mathbb{E}\{\|\mathbf{v}_{kV}^X\|^2\}}} & \frac{\mathbf{v}_{kH}^X}{\sqrt{\mathbb{E}\{\|\mathbf{v}_{kH}^X\|^2\}}} \\ \sqrt{\rho_{kV}^{\text{dl}}} & 0 \\ 0 & \sqrt{\rho_{kH}^{\text{dl}}} \end{bmatrix}, \quad (51)$$

where $X \in \{\text{MMSE}, \text{ZF}, \text{MR}\}$. The corresponding \mathbf{v}_{kH}^X vectors are given in (37)-(39). In the case of MR precoding, the expectations can be computed in closed form as described in the following lemma.

Lemma 6: If MR precoding with

$$\mathbf{W}_k^{\text{MR}} = \begin{bmatrix} \frac{\hat{\mathbf{h}}_{kV}}{\sqrt{\mathbb{E}\{\|\hat{\mathbf{h}}_{kV}\|^2\}}} & \frac{\hat{\mathbf{h}}_{kH}}{\sqrt{\mathbb{E}\{\|\hat{\mathbf{h}}_{kH}\|^2\}}} \\ \sqrt{\rho_{kV}^{\text{dl}}} & 0 \\ 0 & \sqrt{\rho_{kH}^{\text{dl}}} \end{bmatrix} = \begin{bmatrix} \frac{\sqrt{\rho_{kV}^{\text{dl}}}\hat{\mathbf{h}}_{kV}}{\sqrt{\text{tr}(\mathbf{\Gamma}_k^v)}} & \frac{\sqrt{\rho_{kH}^{\text{dl}}}\hat{\mathbf{h}}_{kH}}{\sqrt{\text{tr}(\mathbf{\Gamma}_k^h)}} \end{bmatrix} \quad (52)$$

is used based on the MMSE estimator, then the achievable SE in (49) can be computed in closed form as

$$R_k^{\text{dl}} = \frac{\tau_c - \tau_p}{\tau_c} \log_2 \left(1 + \frac{\rho_{kV}^{\text{dl}} \text{tr}(\mathbf{\Gamma}_k^v)}{\sum_{l=1}^K \left(\rho_{lV}^{\text{dl}} \frac{\text{tr}(\mathbf{\Gamma}_l^v \mathbf{R}_k^v)}{\text{tr}(\mathbf{\Gamma}_l^v)} + \rho_{lH}^{\text{dl}} \frac{\text{tr}(\mathbf{\Gamma}_l^h \mathbf{R}_k^v)}{\text{tr}(\mathbf{\Gamma}_l^h)} \right) + \sigma_{\text{dl}}^2} \right) \\ + \frac{\tau_c - \tau_p}{\tau_c} \log_2 \left(1 + \frac{\rho_{kH}^{\text{dl}} \text{tr}(\mathbf{\Gamma}_k^h)}{\sum_{l=1}^K \left(\rho_{lH}^{\text{dl}} \frac{\text{tr}(\mathbf{\Gamma}_l^h \mathbf{R}_k^h)}{\text{tr}(\mathbf{\Gamma}_l^h)} + \rho_{lV}^{\text{dl}} \frac{\text{tr}(\mathbf{\Gamma}_l^v \mathbf{R}_k^h)}{\text{tr}(\mathbf{\Gamma}_l^v)} \right) + \sigma_{\text{dl}}^2} \right). \quad (53)$$

Proof: The proof follows from direct computation of the expectations and given in Appendix

B. □

The simplified version of (53) for $\mathbf{R}_{\text{BS},k} = \beta_k \mathbf{I}_{\frac{M}{2}}$ for $k = 1, \dots, K$ is

$$R_k^{\text{dl}} = \frac{\tau_c - \tau_p}{\tau_c} \log_2 \left(1 + \frac{\frac{M}{2} \rho_{kV}^{\text{dl}} (\gamma_{kV,1} + \gamma_{kV,2})}{\sum_{l=1}^K \left(\rho_{lV}^{\text{dl}} \frac{\gamma_{lV,1} \beta_k (1 - q_k) + \gamma_{lV,2} \beta_k q_k}{\gamma_{lV,1} + \gamma_{lV,2}} + \rho_{lH}^{\text{dl}} \frac{\gamma_{lV,1} \beta_k q_k + \gamma_{lV,2} \beta_k (1 - q_k)}{\gamma_{lV,1} + \gamma_{lV,2}} \right) + \sigma_{\text{dl}}^2} \right) \\ + \frac{\tau_c - \tau_p}{\tau_c} \log_2 \left(1 + \frac{\frac{M}{2} \rho_{kH}^{\text{dl}} (\gamma_{kH,1} + \gamma_{kH,2})}{\sum_{l=1}^K \left(\rho_{lH}^{\text{dl}} \frac{\gamma_{lH,1} \beta_k (1 - q_k) + \gamma_{lH,2} \beta_k q_k}{\gamma_{lH,1} + \gamma_{lH,2}} + \rho_{lV}^{\text{dl}} \frac{\gamma_{lH,1} \beta_k q_k + \gamma_{lH,2} \beta_k (1 - q_k)}{\gamma_{lH,1} + \gamma_{lH,2}} \right) + \sigma_{\text{dl}}^2} \right). \quad (54)$$

The behavior is similar to as is described in the uplink part.

VI. POWER CONTROL

In this section, we address the problem of maximizing the uplink and downlink sum SEs for MR combining/precoding, based on the new closed-form expressions given in (41) and (54).

A. Uplink Power Control

First, notice that the V/H polarizations give equally strong channels, thus it is desirable to make the uplink pilot powers equal, i.e., $p_l = p_{lV} = p_{lH}$. In this case, the following terms in (41) are symmetric such that

$$\gamma_{l,1} = \gamma_{lV,1} = \gamma_{lH,1} = \frac{p_l \tau_p \beta_l^2 (1 - q_l)^2}{p_l \tau_p \beta_l (1 - q_l) + \sigma_{ul}^2}, \quad (55)$$

$$\gamma_{l,2} = \gamma_{lV,2} = \gamma_{lH,2} = \frac{p_l \tau_p \beta_l^2 q_l^2}{p_l \tau_p \beta_l q_l + \sigma_{ul}^2}. \quad (56)$$

Motivated by the symmetry of the V/H polarizations, the same uplink power should also be used at both polarizations of each UE antenna for data transmission such that $\rho_{lV}^{ul} = \rho_{lH}^{ul} = \rho_l^{ul}$ with $0 \leq \rho_l^{ul} \leq \rho_{tot}^{ul}/2$ for $l = 1, \dots, K$. The maximum uplink transmit power at each UE is ρ_{tot}^{ul} . However, it might not be desired to transmit at maximum power at all UE antennas. Then, we formulate the uplink sum SE maximization problem as

$$\underset{\rho_1^{ul}, \dots, \rho_K^{ul}}{\text{maximize}} \quad \sum_{k=1}^K \frac{2(\tau_c - \tau_p)}{\tau_c} \log_2 \left(1 + \frac{\rho_k^{ul} \frac{M}{2} (\gamma_{k,1} + \gamma_{k,2})}{\sum_{l=1}^K \rho_l^{ul} \beta_l + \sigma_{ul}^2} \right) \quad (57)$$

$$\text{subject to} \quad 0 \leq \rho_l^{ul} \leq \rho_{tot}^{ul}/2, \quad l = 1, \dots, K.$$

The optimization parameters are $\rho_1^{ul}, \dots, \rho_K^{ul}$, while all other terms are constant. The formulation in (57) is non-convex, but we notice that the denominator $\sum_{l=1}^K \rho_l^{ul} \beta_l + \sigma_{ul}^2$ is the same for all UEs. Using this property, we reformulate the problem in convex form similar to [24, Theorem 4] as

$$\begin{aligned} & \underset{x_1, \dots, x_K, s}{\text{maximize}} \quad \sum_{k=1}^K \frac{2(\tau_c - \tau_p)}{\tau_c} \log_2 (1 + a_k^{ul} x_k) \\ & \text{subject to} \quad 0 \leq x_k \leq \frac{s \beta_k \rho_{tot}^{ul}}{2}, \quad k = 1, \dots, K \\ & \quad \quad \quad \sum_{k=1}^K x_k = 1 - \sigma_{ul}^2 s \end{aligned} \quad (58)$$

where $a_k^{\text{ul}} = \frac{M}{2} \frac{\gamma_{k,1} + \gamma_{k,2}}{\beta_k}$, $s = \frac{1}{\sum_{l=1}^K \rho_l^{\text{ul}} \beta_l + \sigma_{\text{ul}}^2}$, $x_k = s \beta_k \rho_k^{\text{ul}}$. Thus, the problems (57) and (58) are equivalent and the solution to (57) can be obtained from the solution of (58) as $\eta_k = \frac{x_k}{s b_k^{\text{ul}}}$. Since we have the convex reformulation (58) we can use any convex solver to find the optimal solutions efficiently. In the numerical results section, we use CVX [25].

B. Downlink Power Control

Similar to the uplink part, motivated by the symmetry of the V/H polarizations, the same downlink power is used for data transmission at both polarizations of each UE antenna such that $\rho_{lV}^{\text{dl}} = \rho_{lH}^{\text{dl}} = \rho_l^{\text{dl}}$ with $\sum_{l=1}^K \rho_l^{\text{dl}} \leq \rho_{\text{tot}}^{\text{dl}}/2$ and $\rho_l^{\text{dl}} \geq 0$ for $l = 1, \dots, K$. The maximum total downlink transmit power at the BS for each polarization is $\rho_{\text{tot}}^{\text{dl}}/2$. Also, the uplink pilot powers are $p_l = p_{lV} = p_{lH}$ as in Section VI-A. Then, we formulate the downlink sum SE maximization problem as

$$\begin{aligned} & \underset{\rho_1^{\text{dl}}, \dots, \rho_K^{\text{dl}}}{\text{maximize}} && \sum_{k=1}^K \frac{2(\tau_c - \tau_p)}{\tau_c} \log_2 \left(1 + \frac{\rho_k^{\text{dl}} \frac{M}{2} (\gamma_{k,1} + \gamma_{k,2})}{\beta_k \sum_{l=1}^K \rho_l^{\text{dl}} + \sigma_{\text{dl}}^2} \right) \\ & \text{subject to} && \sum_{l=1}^K \rho_l^{\text{dl}} \leq \rho_{\text{tot}}^{\text{dl}}/2, \quad l = 1, \dots, K \\ & && \rho_l^{\text{dl}} \geq 0, \quad l = 1, \dots, K. \end{aligned} \quad (59)$$

The optimization parameters are the power allocation coefficients $\rho_1^{\text{dl}}, \dots, \rho_K^{\text{dl}}$ while the other terms are constant. We notice that the sum rate is larger with $(c\rho_1^{\text{dl}}, \dots, c\rho_K^{\text{dl}})$ than with $(\rho_1^{\text{dl}}, \dots, \rho_K^{\text{dl}})$, for any $c \geq 1$. Hence, the solution to (59) must use the maximum power $\sum_{l=1}^K \rho_l^{\text{dl}} = \rho_{\text{tot}}^{\text{dl}}/2$, and we can rewrite the problem as

$$\begin{aligned} & \underset{\eta_1, \dots, \eta_K}{\text{maximize}} && \sum_{k=1}^K \frac{2(\tau_c - \tau_p)}{\tau_c} \log_2 \left(1 + \frac{a_k^{\text{dl}}}{b_k^{\text{dl}} + \sigma_{\text{dl}}^2} \rho_k^{\text{dl}} \right) \\ & \text{s.t.} && \sum_{k=1}^K \rho_k^{\text{dl}} = \rho_{\text{tot}}^{\text{dl}}/2, \quad k = 1, \dots, K \\ & && \rho_k^{\text{dl}} \geq 0, \quad k = 1, \dots, K \end{aligned} \quad (60)$$

where $a_k^{\text{dl}} = \frac{M}{2} (\gamma_{k,1} + \gamma_{k,2})$ and $b_k^{\text{dl}} = \frac{\rho_{\text{tot}}^{\text{dl}} \beta_k}{2}$. The solutions to this reformulated problem can be obtained by water-filling power allocation as $\rho_k^{\text{dl}} = \max \left(\mu - \frac{1+b_k^{\text{dl}}}{a_k^{\text{dl}}}, 0 \right)$ where μ is selected such that $\sum_{k=1}^K \rho_k^{\text{dl}} = \rho_{\text{tot}}^{\text{dl}}/2$. This is also the solution to (59).

VII. NUMERICAL RESULTS

In this section, we evaluate the performance of dual-polarized antennas under different channel conditions. We consider a single-cell massive MIMO network with $\frac{M}{2}$ dual-polarized antennas and $K = 10$ UEs. The UEs are independently and uniformly distributed within a square of size $0.5 \times 0.5 \text{ km}^2$ at distances larger than 15 m from the BS. The BS is located at the center of the cell. The location of each UE is used when computing the large-scale fading and nominal angle between the UEs and BS.

The BS is equipped with a ULA with half-wavelength antenna spacing. For the spatial correlation matrices, we consider $N = 6$ scattering clusters and the covariance matrix of each cluster is modeled by the (approximate) Gaussian local scattering model [26] such that

$$[\mathbf{R}_{\text{BS},k}]_{s,m} = \frac{\beta_k}{N} \sum_{n=1}^N e^{j\pi(s-m)\sin(\varphi_{k,n})} e^{-\frac{\sigma_\varphi^2}{2}(\pi(s-m)\cos(\varphi_{k,n}))^2}, \quad (61)$$

where β_k is the large-scale fading coefficient and $\varphi_{k,n} \sim \mathcal{U}[\varphi_k - 40^\circ, \varphi_k + 40^\circ]$ is the nominal angle of arrival (AoA) for the n cluster. The multipath components of a cluster have Gaussian distributed AoAs, distributed around the nominal AoA with the angular standard deviation (ASD) $\sigma_\varphi = 5^\circ$. The large-scale fading coefficient is modeled (in dB) as

$$\beta_k = -35.3 - 37.6 \log_{10} \left(\frac{d_k}{1\text{m}} \right) + F_k, \quad (62)$$

where d_k is the distance between the BS and UE k , $F_k \sim \mathcal{N}(0, \sigma_{\text{sf}}^2)$ is the shadow fading with $\sigma_{\text{sf}} = 7$.

We consider communication over a 20 MHz channel and the total receiver noise power is -94 dBm. Each coherence block consists of $\tau_c = 200$ samples and $\tau_p = 2K = 20$ pilots are allocated for channel estimation. Unless otherwise stated, equal power allocation is applied such that the pilot powers are $p_{kV} = p_{kH} = 100$ mW and the uplink and downlink transmit powers are $\rho_{kV}^{\text{ul}} = \rho_{kH}^{\text{ul}} = \rho_{kV}^{\text{dl}} = \rho_{kH}^{\text{dl}} = 100$ mW for every UE $k = 1, \dots, K$. Also, $\rho_{\text{tot}}^{\text{ul}} = 200$ mW and $\rho_{\text{tot}}^{\text{dl}} = 2K \times 100$ mW. The XPD value is 5 dB for all UEs.

1) Performance Comparison of Different Combining/Precoding Schemes: In Fig. 1, the uplink sum SE of MMSE-SIC and UaTF bound with MMSE, ZF and MR detectors are shown. The SEs are averaged over different UE locations and shadow fading realizations. The highest SE is achieved by using MMSE-SIC scheme, as expected. Yet, the linear MMSE scheme achieves a competitive uplink sum SE. It shows that a linear detector can reach most of the SE from employing a dual polarized antenna at the UE side. We also observe that the performance

achieved with the MMSE and ZF combining vectors are significantly better than MR. It is because of the fact that the MR combining vector does not have the ability to cancel inter-stream interference. Fig. 2 shows the downlink sum SE for the MMSE, ZF and MR precoders. The solid lines denote the cases where the UEs apply MMSE-SIC to the received data streams, whereas the dashed lines are for the linear MMSE combining. At each UE, MMSE-SIC detection is applied to the two data streams that are received by the orthogonally polarized antennas. The MMSE-SIC and linear MMSE schemes give the same performance due to the lack of polarization correlation between the received data streams.

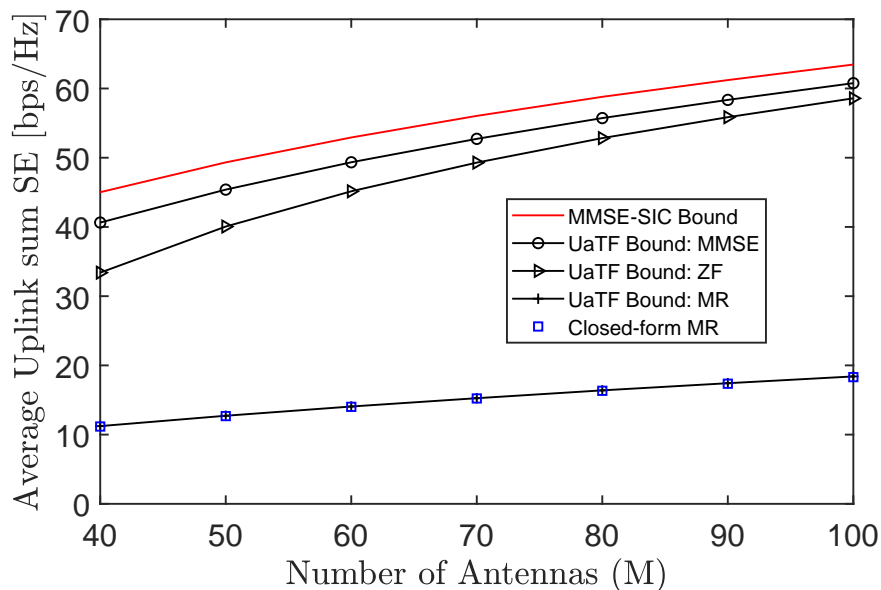


Fig. 1. Average uplink sum SE for 10 UEs with different combining schemes.

2) *Dual-Polarized vs Uni-Polarized Antennas*: Fig. 3 and Fig. 4 compare the sum downlink SEs with dual-polarized and uni-polarized antennas. The number of antennas at the BS and each UE in the uni-polarized setup is M_{uni} and 1, respectively. For $M_{\text{uni}} = \frac{M}{2}$, the H polarized antennas are removed from the dual-polarized antenna arrays both at the BS and UE sides. Therefore, the number of antennas are halved whereas the total array aperture remains the same in both setups. Similarly, for $M_{\text{uni}} = M$, the array is made of only V polarized antennas. Thus, the total array aperture is twice as compared to the dual-polarized setup.

We consider MMSE, ZF and MR precoding for both antenna setups. For the dual-polarized case, MMSE-SIC decoding at the UE side is considered. In the uni-polarized antenna setup, we implemented the MMSE, ZF and MR precoding vectors as

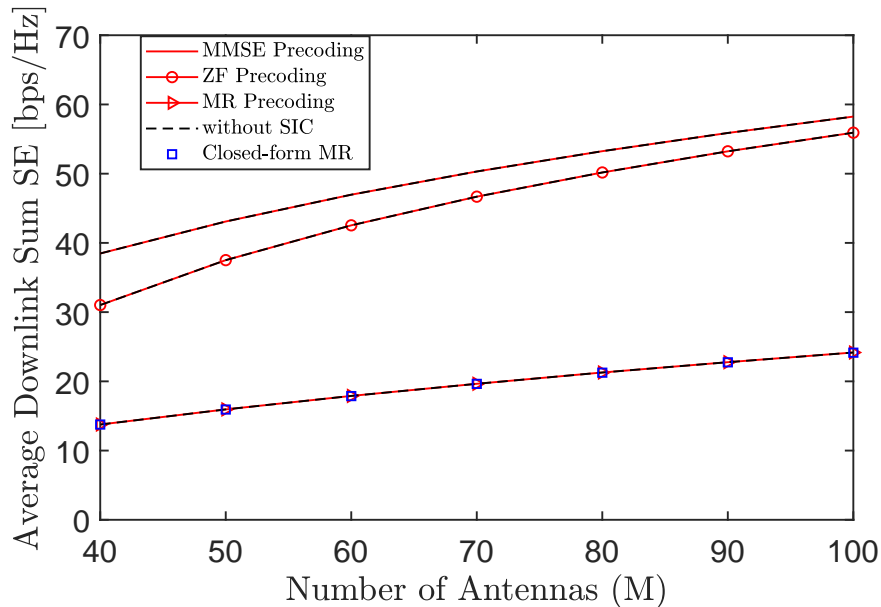


Fig. 2. Average downlink sum SE for 10 UEs with different precoding schemes.

$$\mathbf{W}_k^{\text{uni,MMSE}} = \frac{\sqrt{\rho_{\text{uni}}^{\text{dl}}} \left(\sum_{l=1}^K \rho_{\text{uni}}^{\text{ul}} \hat{\mathbf{h}}_l \hat{\mathbf{h}}_l^H + \rho_{\text{uni}}^{\text{ul}} \mathbf{C}_l + \sigma_{\text{ul}}^2 \mathbf{I}_{M_{\text{uni}}} \right)^{-1} \hat{\mathbf{h}}_k}{\sqrt{\mathbb{E} \left\{ \left\| \left(\sum_{l=1}^K \rho_{\text{uni}}^{\text{ul}} \hat{\mathbf{h}}_l \hat{\mathbf{h}}_l^H + \rho_{\text{uni}}^{\text{ul}} \mathbf{C}_l + \sigma_{\text{ul}}^2 \mathbf{I}_{M_{\text{uni}}} \right)^{-1} \hat{\mathbf{h}}_k \right\|^2 \right\}}}, \quad (63)$$

$$\mathbf{W}_k^{\text{uni,ZF}} = \frac{\sqrt{\rho_{\text{uni}}^{\text{dl}}} [\mathbf{W}_{\text{uni,all}}]_k}{\sqrt{\mathbb{E} \left\{ \left\| [\mathbf{W}_{\text{uni,all}}]_k \right\|^2 \right\}}}, \quad (64)$$

$$\mathbf{W}_k^{\text{uni}} = \frac{\sqrt{\rho_{\text{uni}}^{\text{dl}}} \hat{\mathbf{h}}_k}{\sqrt{\mathbb{E} \left\{ \left\| \hat{\mathbf{h}}_k \right\|^2 \right\}}}, \quad (65)$$

where $\mathbf{W}_{\text{uni,all}} = \mathbf{H}_{\text{uni,all}} (\mathbf{H}_{\text{uni,all}}^H \mathbf{H}_{\text{uni,all}})^{-1}$, $\mathbf{H}_{\text{uni,all}} = [\hat{\mathbf{h}}_1, \dots, \hat{\mathbf{h}}_k, \dots, \hat{\mathbf{h}}_K] \in \mathbb{C}^{M_{\text{uni}} \times K}$. The precoding vectors are generated based on the MMSE estimates of channels $\mathbf{h}_k \sim \mathcal{N}_{\mathbb{C}}(\mathbf{0}, \mathbf{R}_{\text{BS},k})$ as $\hat{\mathbf{h}}_k \sim \mathcal{N}_{\mathbb{C}}(\mathbf{0}, p_{\text{uni}} \tau_{\text{uni,p}} \mathbf{R}_{\text{BS},k} \boldsymbol{\Psi}_k \mathbf{R}_{\text{BS},k})$ with $\boldsymbol{\Psi}_k = (p_{\text{uni}} \tau_{\text{uni,p}} \mathbf{R}_{\text{BS},k} + \sigma_{\text{ul}}^2 \mathbf{I}_{M_{\text{uni}}})^{-1}$ and \mathbf{C}_k is the estimation error covariance matrix, see [3, Sec. 4] for the details. To have a fair comparison, we set $p_{\text{uni}} = \rho_{\text{uni}}^{\text{ul}} = \rho_{\text{uni}}^{\text{dl}} = 200$ mW if $M_{\text{uni}} = \frac{M}{2}$ and $p_{\text{uni}} = \rho_{\text{uni}}^{\text{ul}} = \rho_{\text{uni}}^{\text{dl}} = 100$ mW if $M_{\text{uni}} = M$. Besides, $\tau_{\text{uni,p}} = 10$ so that the total power is constant and the pilot lengths are minimized in both setups. The SE expressions from [3, Sec. 4.3] are utilized to calculate the downlink SE with MR precoding for uni-polarized antennas.

By utilizing the two polarization dimensions, the dual-polarized systems can ideally double the multiplexing gain, as the signal-to-noise ratio (SNR) goes to infinity. In Fig. 3, the downlink sum SE with dual-polarized and uni-polarized antenna arrays are depicted where $M_{\text{uni}} = M$ and $p_{\text{uni}} = \rho_{\text{uni}} = 100$ mW. We observe that the dual-polarized setup offers better performance than the uni-polarized setup. The ratios between the average sum SEs of the dual-polarized and uni-polarized setups are approximately 1.5 for MMSE, 1.4 for ZF precoding and 1.3 for MR precoding. In Fig. 4 where $M_{\text{uni}} = M/2$, it is seen that the ratios between the average sum SEs of the dual-polarized and uni-polarized setups are approximately 1.6 for MMSE and ZF precoding and 1.7 MR precoding. Note that the ratio is not equal to 2 because the XPD is finite (meaning that there is a polarization leakage), the SNR is finite, and the prelog factors $(\tau_c - \tau_p)/\tau_c$ and $(\tau_c - \tau_{\text{uni,p}})/\tau_c$ are different since half the numbers of pilots are used to estimate the uni-polarized channels. The fact that the markers overlap with the curves confirms the validity of our analytical results in Lemma 6. The same behaviors are observed in the uplink but are omitted to avoid repetition.

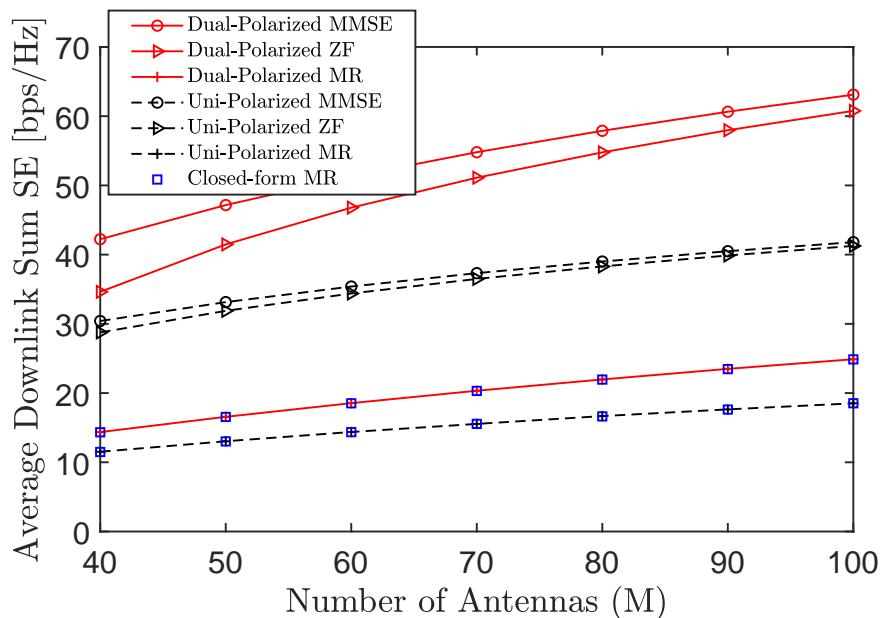


Fig. 3. Average downlink sum SE for 10 UEs with different precoders as a function of the number of BS antennas for dual-polarized and uni-polarized setups with $M_{\text{uni}} = M$ and $p_{\text{uni}} = \rho_{\text{uni}}^{\text{dl}} = 100$ mW.

3) *Effect of Channel Polarization Leakage (XPD)*: Fig. 5 shows the average sum uplink SE for different XPD values. The same XPD values are used across UEs. We observe that the SEs are higher when the polarization leakage is zero (when the XPD is infinite). We observe that the gap

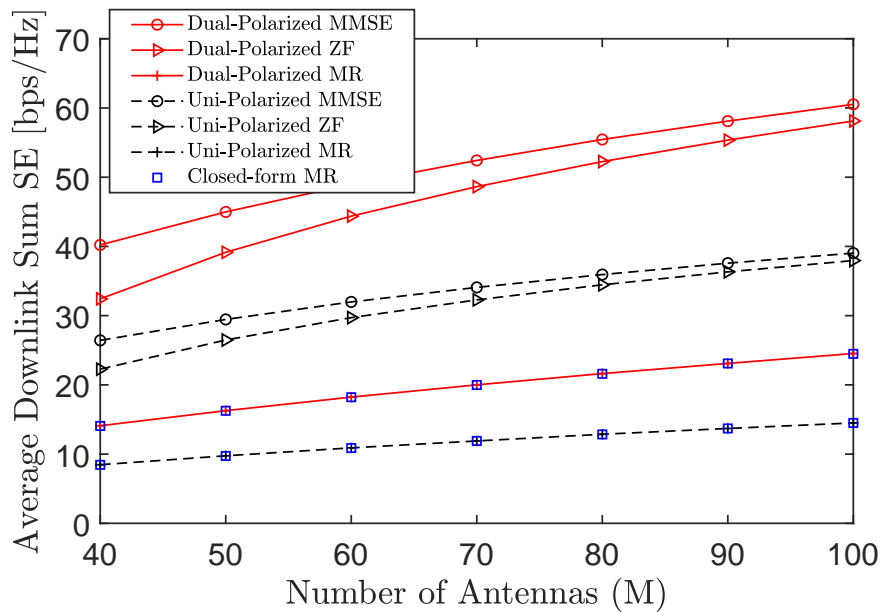


Fig. 4. Average downlink sum SE for 10 UEs with different precoders as a function of the number of BS antennas for dual-polarized and uni-polarized setups with $M_{\text{uni}} = \frac{M}{2}$ and $p_{\text{uni}} = \rho_{\text{uni}}^{\text{dl}} = 200$ mW.

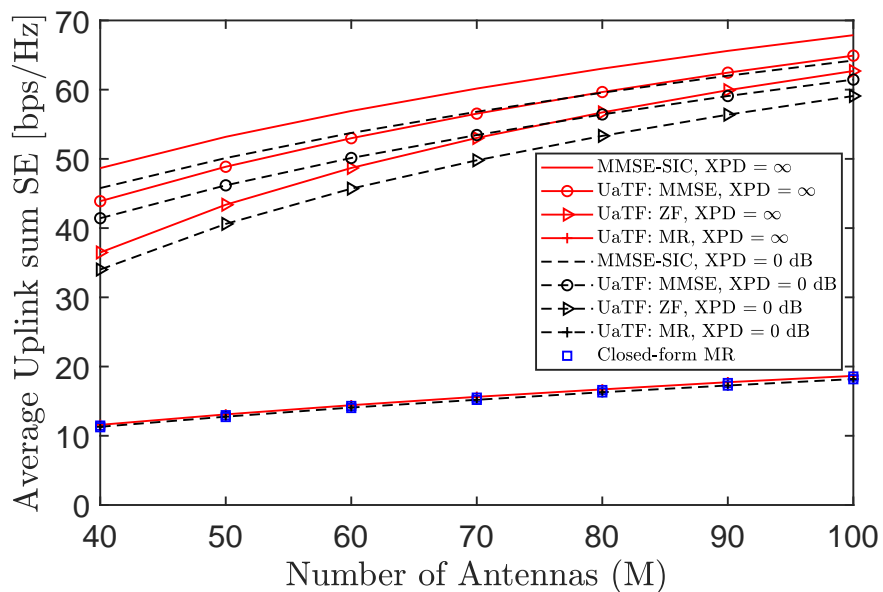


Fig. 5. Average uplink sum SE for 10 UEs with different precoders as a function of the number of BS antennas for different XPD values.

between the MMSE-SIC and linear MMSE increases with the polarization leakage. In Fig. 6, we see the effect of channel XPD on the downlink SEs. Similar to the uplink, the downlink SEs are higher when the XPD is infinite.

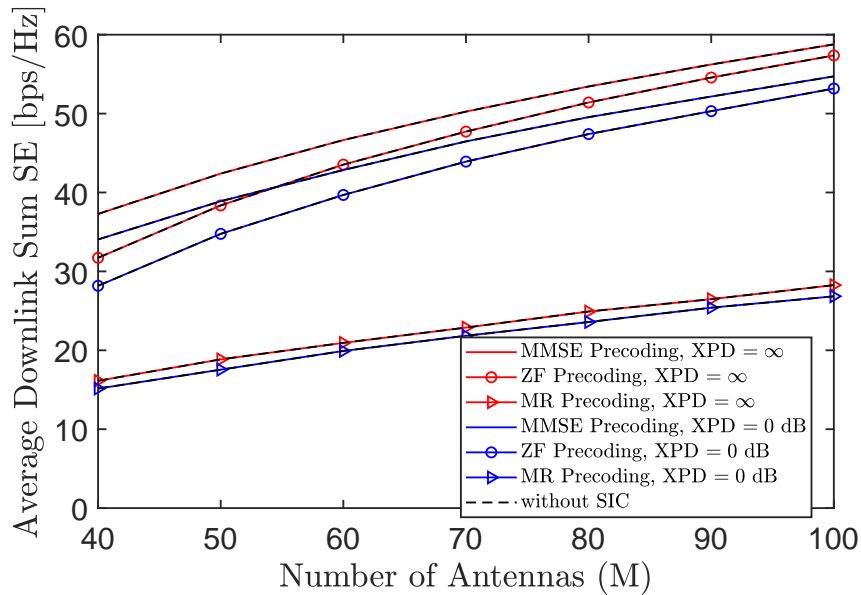


Fig. 6. Average downlink sum SE for 10 UEs with different precoders as a function of the number of BS antennas for different XPD values.

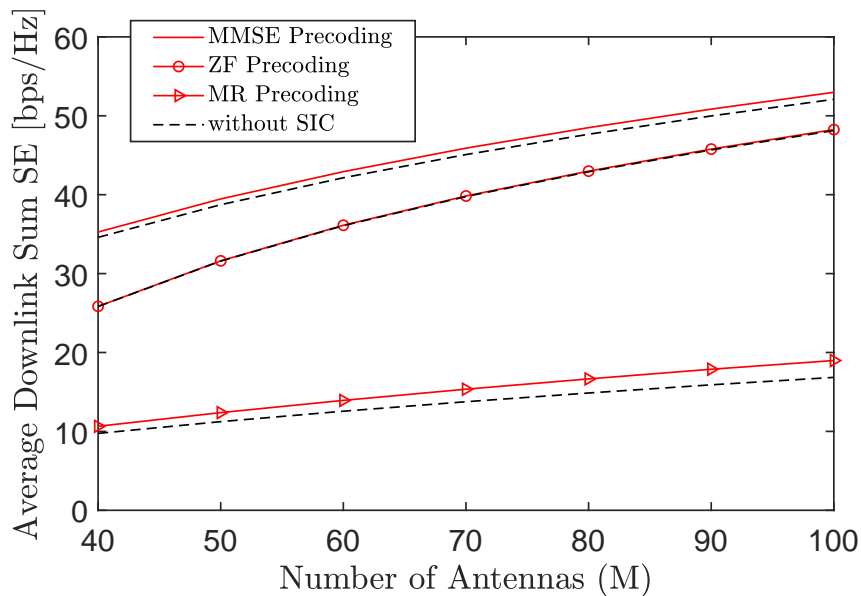


Fig. 7. Average downlink sum SE for 10 UEs where XPC coefficients are $t_p = r_p = 0.8$.

4) *Effect of Polarization Correlations (XPC)*: Fig. 7 shows the average sum downlink SE when the XPC terms at both transmitter and receiver side are set to $t_p = r_p = 0.8$. Notice that they were taken as $t_p = r_p = 0$ in the previous plots. It is seen that there is a gap between the cases with and without SIC, in contrast to Fig. 2 where no polarization correlation is present. Also,

compared to Fig. 2, we observe that a high correlation between the polarized waves reduces the average sum SEs. ZF precoder is the least effected from a nonzero XPC among the precoders.

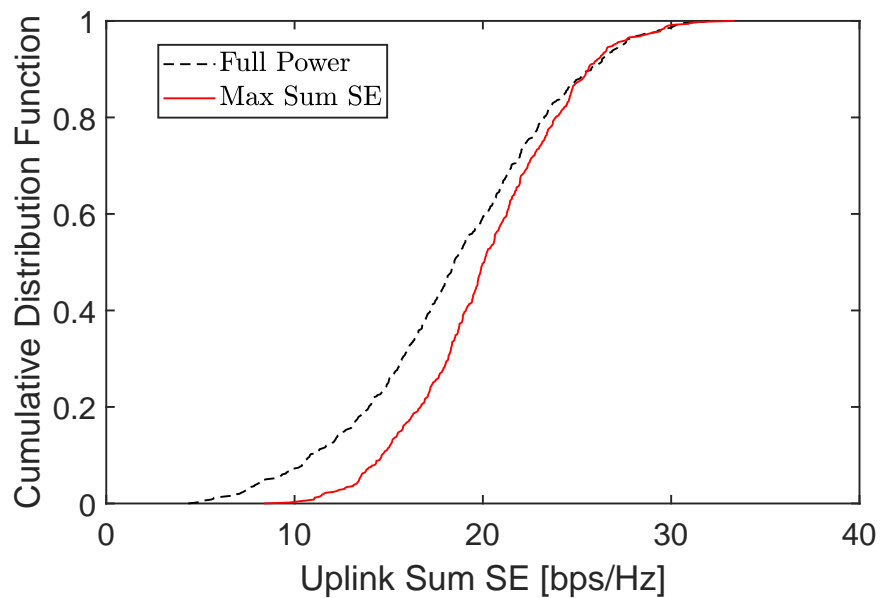


Fig. 8. Cumulative distribution function of uplink sum SE for MR combining scheme with $M = 100$.

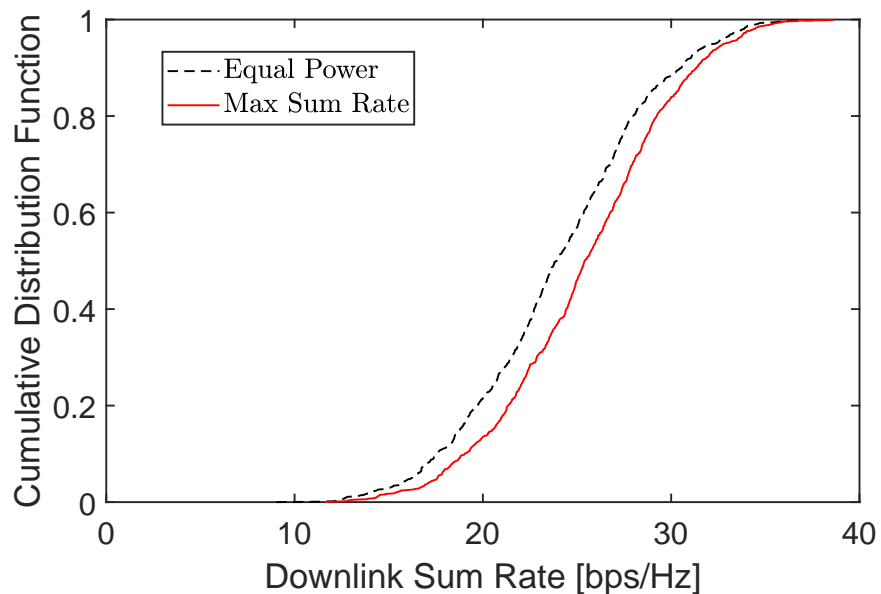


Fig. 9. Cumulative distribution function of downlink sum SE for MR precoding scheme with $M = 100$.

4) *Power Control for Uplink and Downlink SE with MR:* In Fig. 8 and Fig. 9, we compare the sum SE when using equal power allocation (Full Power/Equal Power) and the uplink and

downlink power control schemes for MR combining/precoding (Max Sum SE) that are described in Section VI-A and VI-B, respectively. In the uplink, we observe that the Max Sum SE scheme increases the sum SE compared to the full power scheme. It shows that when some of the UEs cut down their transmit power, it helps to mitigate the interference that they are creating and improves the uplink sum SE. In the downlink, Max Sum SE provides an improvement over the equal power scheme by allocating more power to the better channels and less power to the weaker channels.

VIII. CONCLUSIONS

This paper studied a single-cell massive MIMO system with dual-polarized antennas at both the BS and UEs. We analyzed uplink and downlink achievable SEs with and without SIC for the linear MMSE, ZF and MR combining/precoding schemes. It is observed that the MMSE-SIC scheme gives a better performance in the uplink whereas linear precoding performs the same as MMSE-SIC in the downlink. In addition, we derived the MMSE channel estimator and characterized its statistics. Using the estimates for MR combining/precoding, we computed closed-form uplink and downlink SEs. The SE expressions provide insights into the operation and interference behavior when having dual-polarized channels. Besides, uplink and downlink power control algorithms based on these closed-form expressions are developed.

The dual-polarized and uni-polarized antenna setups are compared numerically. Moreover, the impact of XPD and XPC on uplink and downlink SEs are evaluated. The expression shows how the multiplexing gain can be doubled by utilizing the polarization domain. We observe that dual-polarized arrays have the same physical size and beamforming gain per polarization as a uni-polarized array with half the number of antennas. Hence, the size can be reduced while maintaining or improving the SE.

IX. APPENDIX

A. Proof of Lemma 3

Assume that the signals are decoded in an arbitrary order $x_{1V}, x_{1H}, \dots, x_{KV}, x_{KH}$. First, we can rewrite (32) as

$$\begin{aligned} \mathbf{y} &= \sum_{l=1}^K \sqrt{p_{lV}} \hat{\mathbf{h}}_{lV} x_{lV} + \sqrt{p_{lH}} \hat{\mathbf{h}}_{lH} x_{lH} + \tilde{\mathbf{H}}_l^H \mathbf{P}_l^{1/2} \mathbf{x}_l + \mathbf{n} \\ &= \sqrt{p_{1V}} \hat{\mathbf{h}}_{1V} x_{1V} + \mathbf{n}_{1V}, \end{aligned} \quad (66)$$

where the first signal x_{1V} is transmitted through the effective channel $\sqrt{p_{1V}}\hat{\mathbf{h}}_{1V}$ that is known at the BS and $\mathbf{n}_{1V} = \mathbf{y} - \sqrt{p_{1V}}\hat{\mathbf{h}}_{1V}x_{1V} = \sum_{l=2}^K \sqrt{p_{lV}}\hat{\mathbf{h}}_{lV}x_{lV} + \sum_{l=1}^K \sqrt{p_{lH}}\hat{\mathbf{h}}_{lH}x_{lH} + \tilde{\mathbf{H}}_l^H \mathbf{P}_l^{1/2} \mathbf{x}_l + \mathbf{n}$ is the uncorrelated colored noise and interference. The noise term \mathbf{n}_{1V} has zero mean and its conditional covariance matrix is

$$\mathbf{\Upsilon}_{1V} = \mathbb{E} \left\{ \mathbf{n}_{1V} \mathbf{n}_{1V}^H | \hat{\mathbf{H}}_1, \dots, \hat{\mathbf{H}}_K \right\} = \sum_{l=2}^K p_{lV} \hat{\mathbf{h}}_{lV} \hat{\mathbf{h}}_{lV}^H + \sum_{l=1}^K p_{lH} \hat{\mathbf{h}}_{lH} \hat{\mathbf{h}}_{lH}^H + p_{lV} \mathbf{C}_l^v + p_{lH} \mathbf{C}_l^h + \sigma_{\text{ul}}^2 \mathbf{I}_M. \quad (67)$$

The first stream x_{1V} is detected using MMSE filter $\mathbf{\Upsilon}_{1V}^{-1} \hat{\mathbf{h}}_{1V}$ where the corresponding instantaneous SNR is $\text{SNR}_{1V} = p_{1V} \hat{\mathbf{h}}_{1V}^H \mathbf{\Upsilon}_{1V}^{-1} \hat{\mathbf{h}}_{1V}$. After decoding x_{1V} , it is removed from the received signal \mathbf{y} . Thus, the next data stream x_{1H} is detected based on

$$\begin{aligned} \mathbf{y} - \sqrt{p_{1V}}\hat{\mathbf{h}}_{1V}x_{1V} &= \sqrt{p_{1H}}\hat{\mathbf{h}}_{1H}x_{1H} + \sum_{l=2}^K \sqrt{p_{lV}}\hat{\mathbf{h}}_{lV}x_{lV} + \sqrt{p_{lH}}\hat{\mathbf{h}}_{lH}x_{lH} + \sum_{l=1}^K \tilde{\mathbf{H}}_l^H \mathbf{P}_l^{1/2} \mathbf{x}_l + \mathbf{n} \\ &= \sqrt{p_{1H}}\hat{\mathbf{h}}_{1H}x_{1H} + \mathbf{n}_{1H} \end{aligned} \quad (68)$$

using the MMSE filter $\mathbf{\Upsilon}_{1H}^{-1} \hat{\mathbf{h}}_{1H}$ where the corresponding instantaneous SNR is $\text{SNR}_{1H} = p_{1H} \hat{\mathbf{h}}_{1H}^H \mathbf{\Upsilon}_{1H}^{-1} \hat{\mathbf{h}}_{1H}$ with

$$\mathbf{\Upsilon}_{1H} = \mathbb{E} \left\{ \mathbf{n}_{1H} \mathbf{n}_{1H}^H | \hat{\mathbf{H}}_1, \dots, \hat{\mathbf{H}}_K \right\} = \sum_{l=2}^K p_{lV} \hat{\mathbf{h}}_{lV} \hat{\mathbf{h}}_{lV}^H + p_{lH} \hat{\mathbf{h}}_{lH} \hat{\mathbf{h}}_{lH}^H + \sum_{l=1}^K p_{lV} \mathbf{C}_l^v + p_{lH} \mathbf{C}_l^h + \sigma_{\text{ul}}^2 \mathbf{I}_M. \quad (69)$$

This process is repeated for all $2K$ signals. The last two signals x_{KV} and x_{KH} are decoded as

$$\begin{aligned} \mathbf{y} - \sum_{l=1}^{K-1} \left(\sqrt{p_{lV}}\hat{\mathbf{h}}_{lV}x_{lV} + \sqrt{p_{lH}}\hat{\mathbf{h}}_{lH}x_{lH} \right) &= \sqrt{p_{KV}}\hat{\mathbf{h}}_{KV}x_{KV} + \sqrt{p_{KH}}\hat{\mathbf{h}}_{KH}x_{KH} + \sum_{l=1}^K \tilde{\mathbf{H}}_l^H \mathbf{P}_l^{1/2} \mathbf{x}_l + \mathbf{n} \\ &= \sqrt{p_{KV}}\hat{\mathbf{h}}_{KV}x_{KV} + \mathbf{n}_{KV} \end{aligned} \quad (70)$$

with

$$\mathbf{\Upsilon}_{KV} = \mathbb{E} \left\{ \mathbf{n}_{KV} \mathbf{n}_{KV}^H | \hat{\mathbf{H}}_1, \dots, \hat{\mathbf{H}}_K \right\} = p_{KH} \hat{\mathbf{h}}_{KH} \hat{\mathbf{h}}_{KH}^H + \sum_{l=1}^K p_{lV} \mathbf{C}_l^v + p_{lH} \mathbf{C}_l^h + \sigma_{\text{ul}}^2 \mathbf{I}_M, \quad (71)$$

and

$$\begin{aligned} \mathbf{y} - \sum_{l=1}^K \sqrt{p_{lV}}\hat{\mathbf{h}}_{lV}x_{lV} + \sum_{l=1}^{K-1} \sqrt{p_{lH}}\hat{\mathbf{h}}_{lH}x_{lH} &= \sqrt{p_{KH}}\hat{\mathbf{h}}_{KH}x_{KH} + \sum_{l=1}^K \tilde{\mathbf{H}}_l^H \mathbf{P}_l^{1/2} \mathbf{x}_l + \mathbf{n} \\ &= \sqrt{p_{KV}}\hat{\mathbf{h}}_{KV}x_{KV} + \mathbf{n}_{KH}, \end{aligned} \quad (72)$$

with

$$\mathbf{\Upsilon}_{KH} = \mathbb{E} \left\{ \mathbf{n}_{KH} \mathbf{n}_{KH}^H \right\} = \sum_{l=1}^K p_{lV} \mathbf{C}_l^v + p_{lH} \mathbf{C}_l^h + \sigma_{\text{ul}}^2 \mathbf{I}_M. \quad (73)$$

Then, the achievable SE of UE k becomes [27, Chapter 8]

$$\begin{aligned} R_k^{\text{ul,SIC}} &= \frac{\tau_c - \tau_p}{\tau_c} \mathbb{E} \left\{ \log_2(1 + p_{kV} \hat{\mathbf{h}}_{kV}^H \mathbf{\Upsilon}_{kV}^{-1} \hat{\mathbf{h}}_{kV}) + \log_2(1 + p_{kH} \hat{\mathbf{h}}_{kH}^H \mathbf{\Upsilon}_{kH}^{-1} \hat{\mathbf{h}}_{kH}) \right\} \\ &\stackrel{(a)}{=} \frac{\tau_c - \tau_p}{\tau_c} \mathbb{E} \left\{ \log_2 \det(p_{kV} \hat{\mathbf{h}}_{kV} \hat{\mathbf{h}}_{kV}^H + \mathbf{\Upsilon}_{kV}) - \log_2 \det(\mathbf{\Upsilon}_{kV}) \right\} \\ &\quad + \frac{\tau_c - \tau_p}{\tau_c} \mathbb{E} \left\{ \log_2 \det(p_{kH} \hat{\mathbf{h}}_{kH} \hat{\mathbf{h}}_{kH}^H + \mathbf{\Upsilon}_{kH}) - \log_2 \det(\mathbf{\Upsilon}_{kH}) \right\} \\ &\stackrel{(b)}{=} \frac{\tau_c - \tau_p}{\tau_c} \mathbb{E} \left\{ \log_2 \det(p_{kV} \hat{\mathbf{h}}_{kV} \hat{\mathbf{h}}_{kV}^H + p_{kH} \hat{\mathbf{h}}_{kH} \hat{\mathbf{h}}_{kH}^H + \mathbf{\Upsilon}_{kH}) - \log_2 \det(\mathbf{\Upsilon}_{kH}) \right\} \\ &= \frac{\tau_c - \tau_p}{\tau_c} \mathbb{E} \left\{ \log_2 \det \left(\mathbf{I}_2 + \mathbf{P}_k \hat{\mathbf{H}}_k \left(\sum_{l=k+1}^K p_{lV} \hat{\mathbf{h}}_{lV} \hat{\mathbf{h}}_{lV}^H + p_{lH} \hat{\mathbf{h}}_{lH} \hat{\mathbf{h}}_{lH}^H + \sum_{l=1}^K p_{lV} \mathbf{C}_l^v + p_{lH} \mathbf{C}_l^h + \sigma_{\text{ul}}^2 \mathbf{I}_M \right)^{-1} \hat{\mathbf{H}}_k^H \right) \right\}, \end{aligned} \quad (74)$$

where $\log_2(1 + \mathbf{x}^H \mathbf{A}^{-1} \mathbf{x}) = \log_2 \det(\mathbf{x} \mathbf{x}^H + \mathbf{A}) - \log_2 \det(\mathbf{A})$ is used in (a). In the step (b), we used $\mathbf{\Upsilon}_{kV} = \mathbf{\Upsilon}_{kH} + p_{kH} \hat{\mathbf{h}}_{kH} \hat{\mathbf{h}}_{kH}^H$. Similarly, the achievable uplink sum SE is

$$\begin{aligned} R^{\text{ul,SIC}} &= \sum_{l=1}^K R_l^{\text{ul,SIC}} = \sum_{l=1}^K \frac{\tau_c - \tau_p}{\tau_c} \mathbb{E} \left\{ \log_2(1 + p_{lV} \hat{\mathbf{h}}_{lV}^H \mathbf{\Upsilon}_{lV}^{-1} \hat{\mathbf{h}}_{lV}) + \log_2(1 + p_{lH} \hat{\mathbf{h}}_{lH}^H \mathbf{\Upsilon}_{lH}^{-1} \hat{\mathbf{h}}_{lH}) \right\} \\ &= \frac{\tau_c - \tau_p}{\tau_c} \mathbb{E} \left\{ \log_2 \det(p_{1V} \hat{\mathbf{h}}_{1V} \hat{\mathbf{h}}_{1V}^H + \mathbf{\Upsilon}_{1V}) - \log_2 \det(\mathbf{\Upsilon}_{KH}) \right\} \\ &= \frac{\tau_c - \tau_p}{\tau_c} \mathbb{E} \left\{ \log_2 \det \left(\sum_{l=1}^K \hat{\mathbf{H}}_l^H \mathbf{P}_l \hat{\mathbf{H}}_l + \mathbf{\Upsilon}_{KH} \right) - \log_2 \det(\mathbf{\Upsilon}_{KH}) \right\} \\ &= \frac{\tau_c - \tau_p}{\tau_c} \mathbb{E} \left\{ \log_2 \det \left(\mathbf{I}_M + \sum_{l=1}^K \hat{\mathbf{H}}_l^H \mathbf{P}_l \hat{\mathbf{H}}_l \left(\sum_{j=1}^K p_{jV} \mathbf{C}_j^v + p_{jH} \mathbf{C}_j^h + \sigma_{\text{ul}}^2 \mathbf{I}_M \right)^{-1} \right) \right\}. \end{aligned} \quad (75)$$

B. Proof of Lemma 6

The MR precoding matrix is $\mathbf{W}_k = \begin{bmatrix} \frac{\sqrt{\rho_{kV}} \hat{\mathbf{h}}_{kV}}{\sqrt{\text{tr}(\mathbf{\Gamma}_k^v)}} & \frac{\sqrt{\rho_{kH}} \hat{\mathbf{h}}_{kH}}{\sqrt{\text{tr}(\mathbf{\Gamma}_k^h)}} \end{bmatrix} = [\mathbf{w}_{kV} \mathbf{w}_{kH}]$. The first expectation to calculate in (49) is

$$\begin{aligned} \mathbb{E} \left\{ \mathbf{H}_k \mathbf{W}_k \right\} &= \mathbb{E} \left\{ \left(\hat{\mathbf{H}}_k + \tilde{\mathbf{H}}_k \right) \mathbf{W}_k \right\} = \mathbb{E} \left\{ \hat{\mathbf{H}}_k \mathbf{W}_k \right\} + \mathbb{E} \left\{ \tilde{\mathbf{H}}_k \mathbf{W}_k \right\} = \mathbb{E} \left\{ \hat{\mathbf{H}}_k \mathbf{W}_k \right\} \\ &= \mathbb{E} \left\{ \begin{bmatrix} \hat{\mathbf{h}}_{kV}^H \\ \hat{\mathbf{h}}_{kH}^H \end{bmatrix} [\mathbf{w}_{kV} \mathbf{w}_{kH}] \right\} = \mathbb{E} \left\{ \begin{bmatrix} \hat{\mathbf{h}}_{kV}^H \mathbf{w}_{kV} & \hat{\mathbf{h}}_{kV}^H \mathbf{w}_{kH} \\ \hat{\mathbf{h}}_{kH}^H \mathbf{w}_{kV} & \hat{\mathbf{h}}_{kH}^H \mathbf{w}_{kH} \end{bmatrix} \right\} = \begin{bmatrix} \sqrt{\rho_{kV} \text{tr}(\mathbf{\Gamma}_k^v)} & 0 \\ 0 & \sqrt{\rho_{kH} \text{tr}(\mathbf{\Gamma}_k^h)} \end{bmatrix}. \end{aligned} \quad (76)$$

Then, the second expectation in (49) is

$$\begin{aligned} \mathbb{E} \left\{ \mathbf{H}_k \sum_{l=1}^K \mathbf{W}_l \mathbf{W}_l^H \mathbf{H}_k^H \right\} &= \mathbb{E} \left\{ \left(\hat{\mathbf{H}}_k + \tilde{\mathbf{H}}_k \right) \sum_{l=1}^K \mathbf{W}_l \mathbf{W}_l^H \left(\hat{\mathbf{H}}_k + \tilde{\mathbf{H}}_k \right)^H \right\} \\ &= \mathbb{E} \left\{ \left(\hat{\mathbf{H}}_k + \tilde{\mathbf{H}}_k \right) \mathbf{W}_k \mathbf{W}_k^H \left(\hat{\mathbf{H}}_k + \tilde{\mathbf{H}}_k \right)^H \right\} + \sum_{\substack{l=1 \\ l \neq k}}^K \mathbb{E} \left\{ \mathbf{H}_k \mathbf{W}_l \mathbf{W}_l^H \mathbf{H}_k^H \right\}. \end{aligned} \quad (77)$$

First, for $l = k$, we have

$$\begin{aligned} \mathbb{E} \left\{ \hat{\mathbf{H}}_k \mathbf{W}_k \mathbf{W}_k^H \hat{\mathbf{H}}_k^H \right\} &= \mathbb{E} \left\{ \begin{bmatrix} \hat{\mathbf{h}}_{kV}^H \mathbf{w}_{kV} & \hat{\mathbf{h}}_{kV}^H \mathbf{w}_{kH} \\ \hat{\mathbf{h}}_{kH}^H \mathbf{w}_{kV} & \hat{\mathbf{h}}_{kH}^H \mathbf{w}_{kH} \end{bmatrix} \begin{bmatrix} \hat{\mathbf{h}}_{kV}^H \mathbf{w}_{kV} & \hat{\mathbf{h}}_{kV}^H \mathbf{w}_{kH} \\ \hat{\mathbf{h}}_{kH}^H \mathbf{w}_{kV} & \hat{\mathbf{h}}_{kH}^H \mathbf{w}_{kH} \end{bmatrix}^H \right\} \\ &= \begin{bmatrix} \mathbb{E} \left\{ \left| \hat{\mathbf{h}}_{kV}^H \mathbf{w}_{kV} \right|^2 + \left| \hat{\mathbf{h}}_{kV}^H \mathbf{w}_{kH} \right|^2 \right\} & 0 \\ 0 & \mathbb{E} \left\{ \left| \hat{\mathbf{h}}_{kH}^H \mathbf{w}_{kH} \right|^2 + \left| \hat{\mathbf{h}}_{kH}^H \mathbf{w}_{kV} \right|^2 \right\} \end{bmatrix}, \end{aligned} \quad (78)$$

where

$$\mathbb{E} \left\{ \left| \hat{\mathbf{h}}_{kV}^H \hat{\mathbf{h}}_{kV} \right|^2 \right\} = |\text{tr}(\mathbf{\Gamma}_k^v)|^2 + \text{tr}(\mathbf{\Gamma}_k^v \mathbf{\Gamma}_k^v) = |\text{tr}(\mathbf{\Gamma}_k^v)|^2 + \text{tr}(\mathbf{\Gamma}_k^v (\mathbf{R}_k^v - \mathbf{C}_k^v)), \quad (79)$$

$$\mathbb{E} \left\{ \left| \hat{\mathbf{h}}_{kV}^H \hat{\mathbf{h}}_{kH} \right|^2 \right\} = \mathbb{E} \left\{ \left| \hat{\mathbf{h}}_{kH}^H \hat{\mathbf{h}}_{kV} \right|^2 \right\} = \text{tr}(\mathbf{\Gamma}_k^v \mathbf{\Gamma}_k^h) = \text{tr}(\mathbf{\Gamma}_k^v (\mathbf{R}_k^h - \mathbf{C}_k^h)) = \text{tr}(\mathbf{\Gamma}_k^h (\mathbf{R}_k^v - \mathbf{C}_k^v)), \quad (80)$$

$$\mathbb{E} \left\{ \left| \hat{\mathbf{h}}_{kH}^H \hat{\mathbf{h}}_{kH} \right|^2 \right\} = |\text{tr}(\mathbf{\Gamma}_k^h)|^2 + \text{tr}(\mathbf{\Gamma}_k^h \mathbf{\Gamma}_k^h) = |\text{tr}(\mathbf{\Gamma}_k^h)|^2 + \text{tr}(\mathbf{\Gamma}_k^h (\mathbf{R}_k^h - \mathbf{C}_k^h)). \quad (81)$$

For $l = k$, the estimation error related part is

$$\mathbb{E} \left\{ \tilde{\mathbf{H}}_k \mathbf{W}_k \mathbf{W}_k^H \tilde{\mathbf{H}}_k^H \right\} = \begin{bmatrix} \mathbb{E} \left\{ \left| \tilde{\mathbf{h}}_{kV}^H \mathbf{w}_{kV} \right|^2 + \left| \tilde{\mathbf{h}}_{kV}^H \mathbf{w}_{kH} \right|^2 \right\} & 0 \\ 0 & \mathbb{E} \left\{ \left| \tilde{\mathbf{h}}_{kH}^H \mathbf{w}_{kH} \right|^2 + \left| \tilde{\mathbf{h}}_{kH}^H \mathbf{w}_{kV} \right|^2 \right\} \end{bmatrix} \quad (82)$$

$$\text{with } \mathbb{E} \left\{ \left| \tilde{\mathbf{h}}_{kV}^H \hat{\mathbf{h}}_{kV} \right|^2 \right\} = \text{tr}(\mathbf{\Gamma}_k^v \mathbf{C}_k^v), \mathbb{E} \left\{ \left| \tilde{\mathbf{h}}_{kV}^H \hat{\mathbf{h}}_{kH} \right|^2 \right\} = \text{tr}(\mathbf{\Gamma}_k^h \mathbf{C}_k^v), \mathbb{E} \left\{ \left| \tilde{\mathbf{h}}_{kH}^H \hat{\mathbf{h}}_{kV} \right|^2 \right\} = \text{tr}(\mathbf{\Gamma}_k^v \mathbf{C}_k^h)$$

and $\mathbb{E} \left\{ \left| \tilde{\mathbf{h}}_{kH}^H \hat{\mathbf{h}}_{kH} \right|^2 \right\} = \text{tr}(\mathbf{\Gamma}_k^h \mathbf{C}_k^h)$. Putting them together gives the result

$$\mathbb{E} \left\{ \mathbf{H}_k \mathbf{W}_k \mathbf{W}_k^H \mathbf{H}_k^H \right\} = \begin{bmatrix} \rho_{kV} \text{tr}(\mathbf{\Gamma}_k^v) + \frac{\rho_{kV} \text{tr}(\mathbf{\Gamma}_k^v \mathbf{R}_k^v)}{\text{tr}(\mathbf{\Gamma}_k^v)} + \frac{\rho_{kH} \text{tr}(\mathbf{\Gamma}_k^h \mathbf{R}_k^v)}{\text{tr}(\mathbf{\Gamma}_k^h)} & 0 \\ 0 & \rho_{kH} \text{tr}(\mathbf{\Gamma}_k^h) + \frac{\rho_{kH} \text{tr}(\mathbf{\Gamma}_k^h \mathbf{R}_k^h)}{\text{tr}(\mathbf{\Gamma}_k^h)} + \frac{\rho_{kV} \text{tr}(\mathbf{\Gamma}_k^v \mathbf{R}_k^h)}{\text{tr}(\mathbf{\Gamma}_k^v)} \end{bmatrix}. \quad (83)$$

For $l \neq k$, we have

$$\mathbb{E} \left\{ \hat{\mathbf{H}}_k \mathbf{W}_l \mathbf{W}_l^H \hat{\mathbf{H}}_k^H \right\} = \mathbb{E} \left\{ \begin{bmatrix} \left| \hat{\mathbf{h}}_{kV}^H \mathbf{w}_{lV} \right|^2 + \left| \hat{\mathbf{h}}_{kV}^H \mathbf{w}_{lH} \right|^2 & 0 \\ 0 & \left| \hat{\mathbf{h}}_{kH}^H \mathbf{w}_{lH} \right|^2 + \left| \hat{\mathbf{h}}_{kH}^H \mathbf{w}_{lV} \right|^2 \end{bmatrix} \right\}, \quad (84)$$

where

$$\mathbb{E} \left\{ \left| \hat{\mathbf{h}}_{kV}^H \hat{\mathbf{h}}_{lV} \right|^2 \right\} = \text{tr}(\mathbf{\Gamma}_l^v (\mathbf{R}_k^v - \mathbf{C}_k^v)), \mathbb{E} \left\{ \left| \hat{\mathbf{h}}_{kV}^H \hat{\mathbf{h}}_{lH} \right|^2 \right\} = \text{tr}(\mathbf{\Gamma}_l^h (\mathbf{R}_k^v - \mathbf{C}_k^v)), \mathbb{E} \left\{ \left| \hat{\mathbf{h}}_{kH}^H \hat{\mathbf{h}}_{lV} \right|^2 \right\} = \text{tr}(\mathbf{\Gamma}_l^v (\mathbf{R}_k^h - \mathbf{C}_k^h)), \text{ and } \mathbb{E} \left\{ \left| \hat{\mathbf{h}}_{kH}^H \hat{\mathbf{h}}_{lH} \right|^2 \right\} = \text{tr}(\mathbf{\Gamma}_l^h (\mathbf{R}_k^h - \mathbf{C}_k^h)). \text{ Also, for } l \neq k \text{ the estimation error related part is}$$

$$\mathbb{E} \left\{ \tilde{\mathbf{H}}_k \mathbf{W}_l \mathbf{W}_l^H \tilde{\mathbf{H}}_k^H \right\} = \mathbb{E} \left\{ \begin{bmatrix} \left| \tilde{\mathbf{h}}_{kV}^H \mathbf{w}_{lV} \right|^2 + \left| \tilde{\mathbf{h}}_{kV}^H \mathbf{w}_{lH} \right|^2 & 0 \\ 0 & \left| \tilde{\mathbf{h}}_{kH}^H \mathbf{w}_{lH} \right|^2 + \left| \tilde{\mathbf{h}}_{kH}^H \mathbf{w}_{lV} \right|^2 \end{bmatrix} \right\} \quad (85)$$

$$\text{with } \mathbb{E} \left\{ \left| \tilde{\mathbf{h}}_{kV}^H \hat{\mathbf{h}}_{lV} \right|^2 \right\} = \text{tr}(\mathbf{\Gamma}_l^v \mathbf{C}_k^v), \mathbb{E} \left\{ \left| \tilde{\mathbf{h}}_{kV}^H \hat{\mathbf{h}}_{lH} \right|^2 \right\} = \text{tr}(\mathbf{\Gamma}_l^h \mathbf{C}_k^v), \mathbb{E} \left\{ \left| \tilde{\mathbf{h}}_{kH}^H \hat{\mathbf{h}}_{lV} \right|^2 \right\} = \text{tr}(\mathbf{\Gamma}_l^v \mathbf{C}_k^h), \mathbb{E} \left\{ \left| \tilde{\mathbf{h}}_{kH}^H \hat{\mathbf{h}}_{lH} \right|^2 \right\} = \text{tr}(\mathbf{\Gamma}_l^h \mathbf{C}_k^h). \text{ Arranging the terms for the case } l \neq k \text{ gives}$$

$$\mathbb{E} \left\{ \mathbf{H}_k \mathbf{W}_l \mathbf{W}_l^H \mathbf{H}_k^H \right\} = \begin{bmatrix} \frac{\rho_{lV} \text{tr}(\mathbf{\Gamma}_l^v \mathbf{R}_k^v)}{\text{tr}(\mathbf{\Gamma}_l^v)} + \frac{\rho_{lH} \text{tr}(\mathbf{\Gamma}_l^h \mathbf{R}_k^v)}{\text{tr}(\mathbf{\Gamma}_l^h)} & 0 \\ 0 & \frac{\rho_{lH} \text{tr}(\mathbf{\Gamma}_l^h \mathbf{R}_k^h)}{\text{tr}(\mathbf{\Gamma}_l^h)} + \frac{\rho_{lV} \text{tr}(\mathbf{\Gamma}_l^v \mathbf{R}_k^h)}{\text{tr}(\mathbf{\Gamma}_l^v)} \end{bmatrix}. \quad (86)$$

Substituting these terms into (49) gives the result in Lemma 6.

REFERENCES

- [1] E. G. Larsson, F. Tufvesson, O. Edfors, and T. L. Marzetta, "Massive MIMO for next generation wireless systems," *IEEE Commun. Mag.*, vol. 52, no. 2, pp. 186–195, 2014.
- [2] H. Asplund, D. Astely, P. von Butovitsch, T. Chapman, M. Frenne, F. Ghasemzadeh, M. Hagström, B. Hogan, G. Jöngren, J. Karlsson, F. Kronstedt, and E. Larsson, *Advanced Antenna Systems for 5G Network Deployments*. Academic Press, 2020.
- [3] E. Björnson, J. Hoydis, and L. Sanguinetti, "Massive MIMO networks: Spectral, energy, and hardware efficiency," *Foundations and Trends® in Signal Processing*, vol. 11, no. 3-4, pp. 154–655, 2017.
- [4] M. Shafi, M. Zhang, A. Moustakas, P. Smith, A. Molisch, F. Tufvesson, and S. Simon, "Polarized MIMO channels in 3-D: Models, measurements and mutual information," *IEEE J. Sel. Areas Commun.*, vol. 24, pp. 514–527, 2006.
- [5] G. Calcev, D. Chizhik, B. Goransson, S. Howard, H. Huang, A. Kogiantis, A. F. Molisch, A. L. Moustakas, D. Reed, and H. Xu, "A wideband spatial channel model for system-wide simulations," *IEEE Trans. Veh. Technol.*, vol. 56, no. 2, pp. 389–403, 2007.
- [6] M. Coldrey, "Modeling and capacity of polarized MIMO channels," in *IEEE Vehicular Technology Conference (VTC Spring)*. IEEE, 2008, pp. 440–444.
- [7] C. Oestges, B. Clerckx, M. Guillaud, and M. Debbah, "Dual-polarized wireless communications: From propagation models to system performance evaluation," *IEEE Trans. Wireless Commun.*, vol. 7, no. 10, pp. 4019–4031, 2008.

- [8] H. Joung, H.-S. Jo, C. Mun, and J.-G. Yook, "Capacity loss due to polarization-mismatch and space-correlation on MISO channel," *IEEE Trans. Wireless Commun.*, vol. 13, no. 4, pp. 2124–2136, 2014.
- [9] J. Park and B. Clerckx, "Multi-user linear precoding for multi-polarized Massive MIMO system under imperfect CSIT," *IEEE Trans. Wireless Commun.*, vol. 14, no. 5, pp. 2532–2547, 2015.
- [10] X. Yin, S. Gong, S. Wang, and Z. Zhang, "Two timescale robust energy-efficient precoding for dual-polarized MIMO systems," *IEEE Trans. Commun.*, vol. 68, no. 9, pp. 5575–5589, 2020.
- [11] J. Park and B. Clerckx, "Multi-user linear precoding in massively distributed polarized antenna systems under imperfect CSIT," *IEEE Trans. Veh. Technol.*, vol. 69, no. 5, pp. 5268–5280, 2020.
- [12] A. Sousa de Sena, D. Benevides da Costa, Z. Ding, and P. H. J. Nardelli, "Massive MIMO–NOMA networks with multi-polarized antennas," *IEEE Trans. Wireless Commun.*, vol. 18, no. 12, pp. 5630–5642, 2019.
- [13] I. A. Hemadeh, P. Xiao, Y. Kabiri, L. Xiao, V. Fusco, and R. Tafazolli, "Polarization modulation design for reduced RF chain wireless," *IEEE Trans. Commun.*, vol. 68, no. 6, pp. 3890–3907, 2020.
- [14] J. Zhang, K. J. Kim, A. A. Glazunov, Y. Wang, L. Ding, and J. Zhang, "Generalized polarization-space modulation," *IEEE Trans. Commun.*, vol. 68, no. 1, pp. 258–273, 2020.
- [15] M. B. Khalilsarai, T. Yang, S. Haghghatshoar, and G. Caire, "Structured channel covariance estimation for dual-polarized massive MIMO arrays," in *WSA 2020; 24th International ITG Workshop on Smart Antennas*, 2020, pp. 1–6.
- [16] Ö. Özdogan and E. Björnson, "Downlink spectral efficiency of massive MIMO with dual-polarized antennas," in *2021 International ITG Workshop on Smart Antennas (WSA)*, 2021.
- [17] V. Degli-Esposti, V.-M. Kolmonen, E. M. Vitucci, and P. Vainikainen, "Analysis and modeling on co-and cross-polarized urban radio propagation for dual-polarized MIMO wireless systems," *IEEE transactions on antennas and propagation*, vol. 59, no. 11, pp. 4247–4256, 2011.
- [18] H. Asplund, J. Berg, F. Harrysson, J. Medbo, and M. Riback, "Propagation characteristics of polarized radio waves in cellular communications," in *2007 IEEE 66th Vehicular Technology Conference*, 2007, pp. 839–843.
- [19] B. Clerckx and C. Oestges, *MIMO wireless networks: Channels, techniques and standards for multi-antenna, multi-user and multi-cell systems*. Academic Press, 2013.
- [20] P.-S. Kildal, *Foundations of antenna engineering: a unified approach for line-of-sight and multipath*. Artech House, 2015.
- [21] W. L. Stutzman, *Polarization in electromagnetic systems*. Artech house, 2018.
- [22] X. Li, E. Björnson, S. Zhou, and J. Wang, "Massive MIMO with multi-antenna users: When are additional user antennas beneficial?" in *IEEE ICT*, 2016.
- [23] E. Björnson and B. Ottersten, "A framework for training-based estimation in arbitrarily correlated Rician MIMO channels with Rician disturbance," *IEEE Trans. Signal Process.*, vol. 58, no. 3, pp. 1807–1820, 2010.
- [24] H. V. Cheng, E. Björnson, and E. G. Larsson, "Optimal pilot and payload power control in single-cell massive MIMO systems," *IEEE Transactions on Signal Processing*, vol. 65, no. 9, pp. 2363–2378, 2016.
- [25] M. Grant and S. Boyd, "CVX: Matlab software for disciplined convex programming," <http://cvxr.com/cvx>, Apr. 2011.
- [26] Ö. Özdogan, E. Björnson, and E. G. Larsson, "Massive MIMO with spatially correlated rician fading channels," *IEEE Transactions on Communications*, vol. 67, no. 5, pp. 3234–3250, 2019.
- [27] D. Tse and P. Viswanath, *Fundamentals of wireless communications*. Cambridge University Press, 2005.